

Assessing the Impact of Increased Effluent Discharge into Cape Cod Canal

J. Churchill, Dept. Phys. Oceanography, WHOI, Woods Hole, MA 02543 508-289-2807, jchurchill@whoi.edu

G. Cowles, SMAST, UMass Dartmouth, New Bedford, MA 02744 508-910-6397, gcowles@umassd.edu

J. Rheuban, WHOI, Dept. Mar. Chemistry, WHOI, Woods Hole, MA, 02543 508-289-3782, jrheuban@whoi.edu

Final Report

1. Introduction

1a. Background

The Town of Wareham is considering a significant expansion of its wastewater treatment facility (WWTF) that would enable it to serve additional neighborhoods in Bourne, Plymouth, and Wareham. Currently, the treated effluent from the Wareham WWTF is discharged into the Agawam River, a shallow (order 1-m mean depth at high water) branch of the Wareham River. As part of the plan to expand its WWTF, the Town of Wareham is considering relocating its effluent outfall to the western end of Cape Cod Canal, at or near the site of the sewage outfall of the Massachusetts Maritime Academy (MMA; Figure 1). This is deemed to be a more suitable location for effluent discharge than the Agawam River due to the vigorous tidal flows, and attendant tidal flushing, in the canal. The volume of water passing through the canal on a given flood or ebb tide is estimated to vary through the neap-spring cycle over a range of 14-20 billion gallons (see the Appendix for details), which equates to a daily through-canal flow of roughly 56-80 billion gallons (four times the volume passed on each ebb or flood tide).

As part of a feasibility study of the relocation plan, this project component sought to assess the effect that increased effluent discharge through the MMA outfall would have on nutrient concentrations in the vicinity (e.g., in upper Buzzards Bay, Cape Cod Canal and Cape Cod Bay). The fundamental question addressed was **whether or not the projected increase in effluent discharge associated with redirection of the Wareham WWTF output would appreciably raise nutrient concentrations in critical environments near MMA**. Our assessment focused on the impact on total nitrogen (TN) concentrations and was done in two parts. One part entailed using available data to estimate the present distribution of TN in the aquatic environment near MMA. In the second, we used coupled hydrodynamic and plume-tracking models to estimate the additional TN contained in effluent discharged from the redirected Wareham WWTF outfall. In examining the model results, we focused on the area very near (within a few hundred meters) the MMA discharge and on four nearby regions deemed to be of particular importance. These are: Buttermilk Bay, Butler Cove, Onset Bay and the area of Cape Cod Bay near the eastern canal entrance (Figure 2).

1b. Scenarios Considered

In modeling the effluent plume of the redirected Wareham WWTF discharge, we assumed that the discharge would contain TN at a concentration of 3 mg l⁻¹. We considered two rates of volume discharge: 3 and 10 million gallons per day (MGD) (Table 1). These roughly represent estimates of the minimum and maximum volume outflow rates that would be required to accept redirected discharge from the Wareham WWTF and from increased effluent production associated with planned expansion of the sewer systems in Bourne, Wareham and Plymouth. As these daily volumes of effluent discharge are much smaller than the roughly 56-80 billion gallons of daily flow through the canal, one may expect significant dilution of the effluent by the receiving waters in the canal.

The modeling system was also used to estimate the extent to which the present MMA effluent discharge contributes to TN concentrations in the region near MMA. Currently, the MMA WWTF releases effluent with relatively high TN concentrations (order 100 mg l⁻¹) at low flow rates (order 0.03 MGD) (Figure 3). By contrast, the Wareham WWTF currently discharges effluent with much lower TN concentrations (order 3 mg l⁻¹) at a considerably greater flow rate (of roughly 0.75 MGD). In modeling the effluent plume of the current MMA discharge, we set the flow and TN concentration of the discharge to 0.03 MGD and 100 mg l⁻¹, respectively (Table 1). These values are representative of the average monthly discharge for times of full student occupancy in MMA, which tend to be higher than the mean discharge flow and TN concentration of months of low student occupancy (January, February, July and August) (Figure 3).

1c. Report Outline

In the sections to follow, we first describe the data and analysis used to characterize the TN distributions in our designated areas of interest. We then describe the hydrodynamic model used to simulate the flows over the southern Massachusetts coastal zone. The operation of the model and verification of model results are presented. Attention is then directed at the formulation and operation of the model used to track effluent discharged from the MMA outfall. As will be more fully explained, the effluent tracking is done using the velocities generated by the hydrodynamic model. Results of the effluent tracking are then discussed with a focus on the extent to which the projected effluent outflow associated with relocation of the Wareham WWTF discharge increases TN concentrations in the designated areas of interest. We conclude in the final section with a summary of the findings.

2. Background Nutrient Fields

Two sources of data are used to estimate the background concentration of TN in our designated areas of interest. TN concentrations in upper Buzzards Bay are derived from data collected through the Buzzards Bay Coalition's (BBC's) long-term citizen-science monitoring program. As part of this program, water samples are collected by citizen volunteers over the summer months (principally in July and August) during the last three hours of an outgoing tide. The samples are either filtered on site or after

immediate transport to a laboratory. They are then kept on ice and in the dark while transported for further analysis at the Marine Biological Laboratory. Inorganic nutrients, nitrate and nitrite, (NO_3^- and NO_2^-) are analyzed spectrophotometrically by automated Cd reduction (Johnson and Petty, 1983). Ammonium (NH_4^+) is measured using the phenol hypochlorite method (Strickland and Parsons, 1972). Total dissolved nitrogen (TDN; the sum of $\text{NO}_3^- + \text{NO}_2^- + \text{NH}_4^+$) is measured as nitrate following persulfate digestion (D'Elia et al., 1977). Particulate organic nitrogen (PON) is measured by elemental analysis (Sharp, 1974). The program's methods are outlined in a Quality Assurance Project Plan that has been approved by the Massachusetts Department of Environmental Protection and the U.S. Environmental Protection Agency (Williams and Neill, 2014). Yearly averaged TN (sum of TDN and PON) concentrations over 2013-2016 are in the 200-1000 $\mu\text{g l}^{-1}$ range within our designated areas of interest in upper Buzzards Bay (Buttermilk Bay, Butler Cove, Onset Bay), with higher concentrations tending to occur in the upper regions of these areas (Figures 4 and 5).

The data used to estimate the TN background concentration in Cape Cod Bay are from the Center for Coastal Studies water quality monitoring program (www.capecodbay-monitor.org), which since 2006 has collected water quality information from numerous stations in Nantucket and Vineyard Sounds and in Cape Cod Bay. Three of the program's stations are situated in the coastal zone within 10 km of the eastern entrance to Cape Cod Bay (i.e., in our designated area of interest in Cape Cod Bay). The mean (averaged over the last 10 years) TN concentration at these stations ranges between 211 and 384 $\mu\text{g l}^{-1}$ (Figure 6).

To estimate the background concentration in each designated area of interest, we averaged all TN concentrations acquired over 2006-2016 within each area (excluding small tributaries) (Figure 7). The mean concentrations range from 275 (Cape Cod Bay) to 555 $\mu\text{g l}^{-1}$ (Butler Cove) (Table 2, Figure 8).

3. Hydrodynamic Model

As noted in the Introduction, the modeling component of this project was carried out in two parts. In the first, model flows in the coastal region containing the MMA outfall and our designated areas of interest were simulated with a high-resolution hydrodynamic model. The second part entailed using the modeled flow fields generated by the hydrodynamic model to simulate the transport and mixing of effluent discharged at the MMA outfall. In this section, we present details of the hydrodynamic model. Details of the plume tracking model are presented in Section 4.

3.1 Model Description

The hydrodynamic modeling was carried out using the Finite-Volume Community Ocean Model (FVCOM: Chen et al., 2006; Cowles, 2008), an open source model with over 4000 registered users that has been applied in a wide array of coastal and open ocean studies. FVCOM operates by solving the equations of motion on an unstructured grid, with elements that can be aligned with coastline and bathymetric irregularities. To produce a 3-dimensional solution, FVCOM employs a sigma-coordinate system, in which the vertical component of the model domain is divided into a fixed number of layers (20) that

follow changes in model terrain. Layer thickness, for each of the 20 layers, is thus proportional to water depth.

For this project, we utilized a regional FVCOM-based model known as the Southeastern Massachusetts-FVCOM (SEMASS-FVCOM), which includes the Massachusetts and Rhode Island coastal zones as well as Long Island Sound (Figure 9). SEMASS-FVCOM has been employed, and its results extensively evaluated, by co-PIs Cowles and Churchill for recent studies of tidal energy in the Massachusetts coastal zone (Hakim et al., 2013; Cowles et al., 2017) and the dispersal of bay scallop larvae in Buzzards Bay (Liu et al., 2015). Churchill and Cowles are currently using SEMASS-FVCOM in two NOAA-funded studies. One is aimed at assessing the impact of climate change on the delivery of lobster larvae to suitable juvenile habitat off of southern New England. The other is directed at quantifying the impact of municipal sewage discharge on coastal acidification, focusing on effluent released by the towns of New Bedford, Fairhaven and Wareham.

3.2 Grid Setup

To better resolve the hydrodynamic processes in the vicinity of the proposed wastewater outfall and our designated areas of interest, the computational mesh of SEMASS-FVCOM has been refined in Buzzards Bay and Cape Cod Canal. The refined model grid contains 284,305 elements in the horizontal and 20 evenly spaced sigma-layers in the vertical. The horizontal model-grid resolution varies from 5 km over the outer shelf to 50 m along the coastline of Buzzards Bay and within Cape Cod Canal (Figure 10).

The model bathymetry is interpolated from a composite dataset. The majority of the model domain is encompassed by the 3-arcsecond Gulf of Maine bathymetry product (Twomey and Signell, 2013) and the 1/3-arcsecond Nantucket Inundation Digital Elevation Model (NOAA: Eakins et al., 2009). Data from a directed sounding survey are used to specify the bathymetry of the Cape Cod Canal (USACE, 2011). The coastal boundary is derived from a high-resolution (1/2 arc-second) product developed and distributed by the Massachusetts Office of Coastal Zone Management.

3.3 Boundary Forcing

The model is driven at the open boundary by sea surface elevation constructed from the six primary tidal constituents (M_2 , S_2 , N_2 , K_1 , O_1 and M_4). The phase and amplitude of these constituents and the associated regional barotropic response have been extensively evaluated during the course of prior work (Cowles et al., 2017). Values of the salinity and temperature of water flowing into the domain are also set at the open boundary, and specified from a hindcast of a large scale Gulf of Maine / Southern New England FVCOM-GOM model developed by Dr. Changsheng Chen of U. Mass. Dartmouth (NeCOFS, 2017).

3.4 Surface Forcing

At the surface SEMASS-FVCOM is driven by net heat flux and surface wind stress, which are also derived from the regional 30-year FVCOM-GOM hindcast (NECOFS, 2017). The wind field in Buzzards Bay during 2015 (the year of our model run) displays a strong seasonality (Figure 11). The southwest sea breeze dominates the Buzzards Bay wind field from late spring to early fall. By contrast, winds from late fall to early spring are characterized by synoptic events with the strongest wind magnitudes directed from NW and NE. These characteristics of the 2015 wind field are typical of the seasonal wind field in Buzzards Bay (Liu et al., 2015). In addition to utilizing wind and heat flux data to force the model at the surface, the model simulations also employ satellite-derived sea surface temperature (SST) derived from the NOAA 4 km-resolution product. SST is assimilated into the model using a Newtonian relaxation (nudging) approach, which adjusts the modeled SST to best match the observed SST.

3.5 Freshwater Input

Freshwater is input into the model domain at discrete points along the coastal boundary. The locations of the freshwater entry points into Buzzards Bay are based on the watershed delineations of the Buzzards Bay National Estuary Project, which established 32 watersheds draining into the bay. Unfortunately, there is only one long-term record of freshwater influx into the bay, from a gauge in the Paskamansett River in Dartmouth (USGS 01105933). The freshwater flow from the other watersheds is estimated by multiplying the gauged flow of Paskamansett River by the ratio of a given watershed's area to the area of the Paskamansett River watershed. Using this method we estimate that the average freshwater discharge into the Bay in 2015 to be $21.3 \text{ m}^3 \text{ s}^{-1}$, which is 14% below the 20-year annual mean discharge of $25.0 \text{ m}^3 \text{ s}^{-1}$ (Figure 12). Inputs of freshwater from the major rivers outside the Bay (Connecticut, Blackstone, Pawtuxet, Taunton, Neponset, and Charles) are included in the model and are specified from hourly flow data recorded by USGS gauges (available from <https://waterdata.usgs.gov/nwis>).

3.6 Execution and Data Archiving

The model was executed for the period Jan 1, 2015 to Jan 1, 2016 using a time step of two seconds. The execution required 110,000 core-hours of wall time on 2.6 GHz Intel Haswell Xeons. The two-dimensional fields of sea surface height and depth-averaged velocity, and the three-dimensional fields of velocity, temperature, salinity, and the vertical turbulent eddy diffusivity and viscosity were archived at hourly intervals into NetCDF format files. The total dataset (1.5 TB in size) is accessible through the SMAST Thredds server at:

http://www.smast.umassd.edu:8080/thredds/catalog/buzzards/BBC_WW/catalog.html.

3.7 Model Verification

The model validation utilized long-term observational records from upper Buzzards Bay. These included velocity data from fixed ADCPs acquired as part of the NOAA CMIST program (Pruessner et al., 2007), tidal constituents from the National Ocean Service database (NOS, 2016), and a long-term bottom

temperature record near Cleveland Ledge acquired by the Massachusetts Division of Marine Fisheries (see Figure 10 for observation locations).

Sea Surface Elevation

The model simulation of sea surface elevation was compared with the sea surface records from the six National Ocean Service tidal elevation stations (NOS, 2016) within upper Buzzards Bay and the Cape Cod Canal (Figure 10). Surface elevation was extracted from the model hindcast at the grid points nearest each station. Phase and amplitude of the principal regional tidal constituents (M_2 , S_2 , N_2 , K_1 , O_1 and M_4) were then computed from the observed and modeled surface elevation time series using harmonic analysis (T-Tide, Pawlowicz et al., 2002).

The amplitude of the dominant M_2 tide derived from the modeled sea levels is in close agreement, within 3 cm, of the observed M_2 tidal amplitude at all NOS sites except at the Cape Cod Canal Railroad Bridge (5 cm) (Table 3). Within the domain of interest, the M_2 phase rapidly varies due to the differences in the tidal regimes of Cape Cod Bay (reflected by the Canal East station measurements; Table 3) and Buzzards Bay (Nyes Neck). The amplitude and phase of the M_2 tide in Cape Cod Bay differs from M_2 tidal amplitude and phase in Buzzards Bay by, respectively, a factor 2.4 and a lag of 3.5 hours. The model captures these phase and amplitude differences as well as the variation of M_2 phase and amplitude along the Canal (Table 3).

To quantify model skill, the observed and modeled tidal constituents were used to construct an annual time series of tidal elevation at each NOS site. As illustrated by a comparison of modeled and observed tidal records for July 2015 (Figure 13), the modeled tidal elevations are in close agreement with the observations through the complete lunar cycle at all six stations. For skill we selected the root mean square error (RMSE) and the dimensionless Willmott score (Willmott, 1981), which carries the value of 0 (no agreement) to 1 (perfect agreement). RMSE values for the six sites based on the annual time series ranged from 3.4 to 8 cm; whereas Willmott scores ranged from 0.96 to 1.0.

Velocity

The model skill in simulating currents in upper Buzzards Bay was evaluated with water velocity measurements acquired by five bottom-mounted, upward-looking ADCPs deployed for 1-3 months in 2009 of as part of the NOAA CMIST program (Pruessner et al., 2007; see Figure 10 for locations). The ADCP velocity data were archived at 6-min intervals and extend vertically in 1.0-m bins from 2.5 meters above bottom to ~2 m below the surface.

To compare SEMASS-FVCOM velocities with these measurements, the model was run for the duration of the CMIST period (1 June 2009 - 31 July 2009). The depth-averaged modeled and measured velocities are closely aligned in magnitude and phase, with the modeled velocities capturing the diurnal and spring-neap variation of the depth-averaged velocities at all five sites (Figure 14).

The depth-averaged velocity time series were decomposed into the principal tidal constituents (M_2 , S_2 , N_2 , K_1 , O_1 and M_4) using the MATLAB routine T-Tide (Pawlowicz et al., 2002). From these harmonic constituents, annual time series of the tidal flows of both the observed and model-computed currents were reconstructed. Comparison of model- and data-derived vertically averaged tidal flow magnitude at

the five CMIST sites gave Willmott scores ranging from 0.96 to 0.99 and RMSE values from 5 to 25 cm s⁻¹ (Table 4).

The reconstructed time series were used to compare the model- and measurement-derived vertical profiles of mean velocity magnitude at each site. The vertical shear and magnitude of the measurement- and model-derived velocities are in close agreement at CMIST-1 (East entrance of the canal) and at CMIST-5 (just outside the West entrance of the Canal) and CMIST-6 (Abiel's Ledge) (Figure 15). The model under-predicts the mean velocity magnitude in the center of the Canal (by ~ 0.2 m s⁻¹), at CMIST-2 and CMIST-3

At all sites, tidal ellipses computed from the measurement- and model-derived reconstructed time series of depth-averaged currents are in close agreement in both orientation and magnitude (Figure 16).

Based on the above comparison, the model is judged capable of closely reproducing flows in Cape Cod Canal and the upper portion of Buzzards Bay.

4. Plume-Tracking Model

The plume tracking simulations were carried out using the high-resolution three-dimensional velocity fields generated by the hydrodynamic model and focused on the transport and mixing of TN discharged at the MMA outflow (i.e., effluent TN). We did not attempt to model the background concentration of TN. Furthermore, the effluent TN was considered to be conservative. No attempt was made to account for the transformation of effluent TN. As transformational processes would tend to extract effluent TN from the water column (i.e., through transfer through the air-water interface or through biological uptake and transfer to the sediments), the modeled concentrations of effluent TN represent maximum concentrations of TN released at the MMA outfall.

The plume tracking simulations operated by solving the diffusion-advection equation in three dimensions with a source term (applied at the outfall). Denoting the effluent TN concentration as C_E , the equation is expressed as

$$\frac{\partial C_E}{\partial t} = - \left[u \frac{\partial C_E}{\partial x} + v \frac{\partial C_E}{\partial y} + w \frac{\partial C_E}{\partial z} \right] + K_H \left[\frac{\partial^2 C_E}{\partial x^2} + \frac{\partial^2 C_E}{\partial y^2} \right] + K_V \frac{\partial^2 C_E}{\partial z^2} + SS$$

A
B
C
D
E

where: x , y and z are the east, north and vertical coordinates, respectively; t is time; u , v and w are the east, north and vertical velocity components; K_H and K_V are the horizontal and vertical diffusivities; and SS is the source of TN introduced at the outfall.

The solution of the above equation is carried out within model 'tracer' control volumes surrounding each model node (Figure 17). Vertically, each control volume is divided into 20 evenly spaced layers, corresponding to the hydrodynamic model's sigma-layers. Solving for the change in effluent TN concentration (term *A* above) in each layer of each control volume entails determining the advective fluxes (term *B*) of TN through the boundaries of the control volume layer (including through the layer's vertical boundaries), and the diffusive TN fluxes through the layer's horizontal (term *C*) and vertical

(term D) boundaries. The advective fluxes are determined with the velocities output from the hydrodynamic model. In determining the horizontal diffusive fluxes, K_H is set to a uniform value of $0.2 \text{ m}^2 \text{ s}^{-1}$. Values for K_V are taken from the output of the hydrodynamic model (K_V depends on the vertical shear of the horizontal velocity) with a minimum value of $0.3 \times 10^{-2} \text{ m}^2 \text{ s}^{-1}$ imposed.

The input of effluent TN (term E) occurs in the control volume encompassing the outfall (Figure 17) at a rate (mass per unit time) of $V * C_{discharge}$, where $C_{discharge}$ is the concentration of TN emerging from the outfall and V is the volume rate of discharge (i.e., 10 MGD for scenario 3 in Table 1). It is assumed that the discharged TN is initially mixed vertically and horizontally in the control volume containing the outfall (which measures roughly 30x50 m). This is consistent with CTD measurements taken near the outfall (by members of the project team and others) that show little vertical stratification in temperature or salinity. It is assumed that all effluent TN passing through the model's oceanic (open) boundary (Figure 9) is lost to the system (i.e., does not return to the model domain). As the model boundaries are far from our designated areas of interest, this boundary condition has no appreciable effect on the modeled TN concentrations in these areas.

The model was executed in monthly increments for all of 2015. The final concentration field of each month was used as the initial concentration field for the subsequent month. The model time step was set at 20 s. In solving the equation for each time step, the velocities and K_V values output by the hydrodynamic model (at hourly intervals) were interpolated to center of each time step.

The model code was formulated (in MATLAB) by project team members Churchill, Cowles and Rheuban for use in a MIT Sea Grant-funded project aimed at quantifying the impact of municipal effluent discharge on the carbonate system of coastal waters. As part of this project, the code has been subject to considerable testing (i.e., by comparison of modeled and observed effluent concentration patterns). In the simulations for this project, we checked for mass conservation (that the accumulated effluent TN in the model domain equaled the amount discharged plus the amount lost at the open oceanic boundary) and that the concentrations in each region matched the total mass in the region divided by the region's volume.

5. Estimates of Total Nitrogen Added by Effluent Discharge.

Results for the effluent tracking model are described below, focusing separately on the effluent TN concentrations in the area of Cape Cod Canal very near the MMA outfall and on the effluent TN fields in designated areas of interest further from the discharge. In discussing the results, the concentration of effluent TN (i.e., the TN emanating from the discharge, which is separate from the 'background' concentration of TN in the receiving waters) is denoted at C_E (see the above section). The vertical-average of C_E is represented by $\langle C_E \rangle$, whereas the temporal average of $\langle C_E \rangle$ over some time period is denoted as $[\langle C_E \rangle]_T$.

5.1 Added Total Nitrogen near the Discharge Site

Modeled values of $\langle C_E \rangle_T$ reveal a tendency for the concentration of effluent TN to rapidly decline moving away from the outfall (Figure 18). For example, $\langle C_E \rangle_T$ determined for a 10 MGD discharge and averaged over July declines from a maximum of roughly $7 \mu\text{g l}^{-1}$ in the model cell containing the discharge (which measures roughly $30 \times 50 \text{ m}$) to less than $3 \mu\text{g l}^{-1}$ in model cells roughly 100 m up-canal (to the NE) and down-canal (to the SW) of the discharge (Figure 18c). The $\langle C_E \rangle_T$ fields computed for a projected 3 MGD discharge and for the current MMA discharge (Figure 18a,b) show a similar pattern except with reduced $\langle C_E \rangle_T$ (by a factor of 3.33 for the 3 MGD discharge and 10 for the current discharge). Also apparent in all $\langle C_E \rangle_T$ fields is a rapid decline in effluent TN concentration moving away from the outfall in the cross-canal direction. For example, in all monthly $\langle C_E \rangle_T$ fields, the outfall cell concentration is roughly four times higher than the concentration in the cell in the center of the canal directly across from the outfall (e.g. Figure 18).

The rapid decline in $\langle C_E \rangle$ moving away from the outfall is reflected in the field of dilution ratio, defined here as the ratio of the $\langle C_E \rangle_T$ to the TN concentration released at the outfall (3 mg l^{-1} for the projected future discharge). Mathematically, the dilution ratio, D , is defined as

$$D = \frac{C_{discharge}}{\langle C_E \rangle_T}$$

It should be noted that because a change in $C_{discharge}$ will produce a corresponding change in $\langle C_E \rangle_T$, D does not depend on the discharged concentration ($C_{discharge}$) and so is the same for all three discharge scenarios considered (Table 1).

National shellfish sanitation regulations generally prohibit shellfish harvest within the area of a 1000:1 dilution from a WWTF outfall. D fields computed from $\langle C_E \rangle_T$ of each simulation month show the 1000:1 contour tightly confined to the region near the discharge. In the most expansive monthly D field, determined from the $\langle C_E \rangle_T$ of July, the 1000:1 contour spans distances of roughly 45 and 300 m, respectively, in the along- and across-canal directions, and encompasses an area of approximately 0.13 km^2 (Figure 19).

The rapid decline in effluent TN concentration moving away from the outfall is also apparent in the instantaneous values $\langle C_E \rangle$ in the vicinity of the outfall (Figure 20). The modeled $\langle C_E \rangle$ recorded at the outfall exhibits a wide variation linked with the strength of the tidal flow. The outfall TN concentrations (averaged over the model cell (control volume) containing the discharge, Figure 17) are highest (order $50 \mu\text{g l}^{-1}$) during slack tide conditions (at high and low water). During all other tidal phases, $\langle C_E \rangle$ at the outfall is considerably smaller ($<10 \mu\text{g l}^{-1}$). Time series of $\langle C_E \rangle$ at sites $\sim 275 \text{ m}$ up-canal (to the NW) and down-canal of the outfall (sites C1 and C2 in Figure 2) also show considerable tidal modulation. However, the $\langle C_E \rangle$ at these sites peak at maxima of less than $10 \mu\text{g l}^{-1}$.

To illustrate the vertical distribution of $\langle C_E \rangle$ near the outfall, we show here (Figure 21) representative contours of model-computed $\langle C_E \rangle$ along a transect extending across Cape Cod Canal at the canal's western entrance (along line a-b in Figure 2). The $\langle C_E \rangle$ fields are shown for four phases of the tide:

beginning of ebb (high tide), mid-ebb (flow into the canal from Buzzards Bay), beginning of flood, mid-flood (flow into Buzzard Bay). During all tidal phases, there is very little vertical variation of $\langle C_E \rangle$ over the transect, reflecting a high level of vertical mixing in the canal even near peak high and low water levels. The highest $\langle C_E \rangle$ values ($>8 \mu\text{g l}^{-1}$) are seen at the beginning of ebb tide at the northern end of the transect (adjacent to MMA). During mid-ebb and mid-flood, $\langle C_E \rangle$ is consistently low ($<3 \mu\text{g l}^{-1}$) over the full transect. Values of $\langle C_E \rangle$ are consistently low at the southern end of the transect (at the canal shore opposite of MMA), not exceeding $3 \mu\text{g l}^{-1}$.

Assessing the impact of effluent discharge on the TN concentrations near the outfall, requires estimating a background TN concentration (not influenced by the current MMA discharge) in the vicinity of the outfall. The BBC long-term citizen-science monitoring program station with TN measurements closest to the outfall is MMA1, located off the MMA docking facility (Figure 4). To determine if the mean TN concentration of $321 \mu\text{g l}^{-1}$ (standard deviation of $43 \mu\text{g l}^{-1}$) measured at MMA1 is significantly influenced by the current MMA discharge (Table 1), we may use the modeled $\langle C_E \rangle$ in the grid cell containing MMA1. For all months, the average $[\langle C_E \rangle]_T$ computed for the current MMA discharge is no greater than $0.25 \mu\text{g l}^{-1}$. As this is a small fraction ($<0.1\%$) of the mean TN concentration measured at MMA1, we can assume the TN concentrations measured at MMA1 are not influenced by the current discharge. We may thus use the mean TN concentration at MMA1 as the near-outfall background concentration.

The model results indicate that even for the maximum projected volume discharge rate of 10 MGD, the $\langle C_E \rangle$ at the discharge should be small in comparison with the background concentration. During periods of maximum near-outfall TN concentrations (at slack water) the $\langle C_E \rangle$ at the outfall is no more than 17 % of our designated $321 \mu\text{g l}^{-1}$ background concentration (Figure 22b). Averaging across all tidal phases in a month, the maximum monthly mean $[\langle C_E \rangle]_T$ (for July) is $6.7 \mu\text{g l}^{-1}$, or 2 % of the designated background TN concentration.

The ratio of $\langle C_E \rangle$ to the background concentration declines dramatically moving away from the source. At the sites ~ 275 m up-canal (to the NW) and down-canal of the outfall (sites C1 and C2 in Figure 2), $\langle C_E \rangle$ peaks at no greater than 3 % of the background TN concentration (Figure 22a, c). The maximum monthly mean $[\langle C_E \rangle]_T$ at these sites (again in July) is less than 0.7 % of the background. According to these model results, we may conclude that the impact of the projected maximum discharge on TN concentrations near the outfall is minor.

5.2 Added Total Nitrogen in upper Buzzards Bay and Cape Cod Bay

The monthly averaged $[\langle C_E \rangle]_T$ fields show relatively low concentrations over all of upper Buzzards Bay including our designated areas of interest (Buttermilk Bay, Butler Cove, Onset Bay) (Figure 23). For the largest projected discharge rate of 10 MGD, monthly $[\langle C_E \rangle]_T$ averages in these areas do not exceed $3.5 \mu\text{g l}^{-1}$. For the minimum projected discharge rate, the monthly average $[\langle C_E \rangle]_T$ in these areas of importance is less than $1.5 \mu\text{g l}^{-1}$. The tidal variation of $\langle C_E \rangle$ in the designated areas of interest (including Cape Cod Bay) is much smaller than observed near the outfall (compare Figures 20 and 24). The instantaneous values of $\langle C_E \rangle$ in the designated areas of interest in upper Buzzards Bay are consistently below $4 \mu\text{g l}^{-1}$ for the maximum 10 MGD discharge (Figure 24a-c). In Cape Cod Bay, the

instantaneous values of $\langle C_E \rangle$ are even lower, not exceeding $1 \mu\text{g l}^{-1}$ for a 10 MGD discharge (Figure 24d). The model results indicate that C_E tends to be vertically mixed throughout the water column in upper Buzzards Bay, as illustrated by the contoured fields of C_E along a line extending across the upper bay (Figure 25).

To assess the impact of increased TN discharge on the TN concentrations in the designated areas of importance, we compared the averaged measured TN in each area (which may be regarded as the background TN concentration) (Table 2; Figures 7 and 8) to a similar average of the modeled-estimate of the TN added by the discharge. The averages of the modeled added-TN shown here (Table 2, Figure 8) were determined from modeled $\langle C_E \rangle$ fields from May-September (roughly corresponding to the season of the TN measurements in upper Buzzards Bay and Cape Cod Bay). The averages were taken over the full extent of each designated areas (as indicated by the shading in Figure 7).

The results indicate that the projected increased discharge from the MMA facility should negligibly impact TN concentrations in the designated areas of interest. For the maximum 10 MGD discharge, the model-estimated average of additional effluent-TN within the areas of interest in upper Buzzards Bay (Buttermilk Bay, Butler Cove, Onset Bay) is less than 0.5 % of the estimated background TN concentration (Table 2, Figure 8). The impact of effluent-TN is predicted to be even smaller in Cape Cod Bay, where the averaged effluent TN concentrations are close to 0.1 % of the estimated background concentration (Table 2, Figure 8).

The instantaneous values of $\langle C_E \rangle$ in each area of interest are consistently a small fraction of the estimated background concentration, $<1\%$ in Buttermilk Bay, Butler Cove, Onset Bay and $<0.2\%$ in Cape Cod Bay (Figure 26).

A final property to be considered is the seasonal variation of the model-predicted addition to TN due to the projected MMA discharge. Monthly averaged fields of $[\langle C_E \rangle]_T$ (Figure 27) show a seasonal variation likely produced by a variation in the strength of wind-driven currents acting to flush effluent TN out upper Buzzards Bay. The $[\langle C_E \rangle]_T$ fields in upper Buzzards Bay have the lowest values during the winter months (when local wind forcing tends to be directed down-bay; Figure 11) and the highest values during summer months (when local wind-forcing tends to be directed up-bay; Figure 11). Note that in presenting the model findings, we have focused on results from the summer months of the highest effluent TN concentrations in upper Buzzards Bay. In winter months, the impact of the projected discharge on TN concentrations would be even smaller than shown here for the months of July and August (Figures 18-26).

6. Summary

In summarizing, we return to the fundamental question posed in the Introduction of **‘whether or not the projected increase in effluent discharge associated with redirection of the Wareham WWTF output would appreciably raise nutrient concentrations in critical environments near MMA’**. The model results consistently show that the projected discharge of effluent associated with the redirection

of the Wareham WWTF outfall (3 mg l^{-1} TN at 3-10 MGD) will have little effect on the TN concentration in the nearby aquatic environment. Among the notable model findings are:

- The projected effluent discharge will increase the mean monthly TN concentration at the outfall site by an of order 0.6 (3 MGD discharge) to 2 % (10 MGD discharge).
- The instantaneous increase in TN concentration at the outfall due the discharged effluent is greatest during periods of slack/near-slack water, reaching a maximum of 5 % (3 MGD discharge, not shown) to 17 % (10 MGD discharge) of the background TN concentration.
- The concentration of TN discharged from the outfall declines rapidly going away from the outfall. At ~ 275 m up- or down-canal from the outfall, the predicted maximum (at slack water) increase in TN concentration due to the discharge ranges from order 1 (3 MGD discharge) to 3 % (10 MGD discharge) of the background concentration. The increase in mean TN concentration at these distances from the outfall is order 0.2 (3 MGD discharge) to 0.7 % (10 MGD discharge) of the background concentration.
- The predicted increase in TN concentration within designated areas of interest in upper Buzzards Bay (Buttermilk Bay, Butler Cove, Onset Bay) is no more than 1 % (10 MGD discharge) of the background, while the predicted increase in TN concentration in Cape Cod Bay is no more than 0.2 % (10 MGD discharge) of background concentration.
- The region delineated by the 1000:1 dilution contour is roughly 45 m by 300 m around the outfall and encompasses an area of approximately 0.13 km^2

The rapid dilution of effluent predicted by the model reflects the flow conditions at the outfall. A priori, rapid dilution of material discharged into Cape Cod Canal may be expected given the massive volume of water passing through the canal on each tide (on the order of 20 billions gallons).

References

- Chen, C., Beardsley, R., Cowles, G. (2006). An unstructured-grid Finite-Volume Coastal Ocean Model (FVCOM) System, *Oceanography*, 19 (1), 78–89.
- Chen, C., Liu, H., Beardsley, R. C. (2003). An unstructured grid, finite-volume, three-dimensional, primitive equations ocean model: application to coastal ocean and estuaries, *Journal of Atmospheric and Oceanic Technology*, 20 (1), 159–186.
- Cowles, G. W. (2008). Parallelization of the FVCOM coastal ocean model, *International Journal of High Performance Computing Applications*, 22 (2), 177–193.
- Cowles, G.W., Hakim, A., and Churchill, J. H., A comparison of numerical and analytical predictions of the tidal stream power resource of Massachusetts, USA, *Renewable Energy*, in press.
- D’Elia, C. F., and Steudler, P. A. (1977). Determination of total nitrogen in aqueous samples using persulfate digestion, *Limnology and Oceanography*, 22, 760-764.
- Eakins, B. W., Taylor, L. A., Carignan, K. S., Warnken, R. R., Lim, E., Medley, P. R. (2009). Digital elevation model of Nantucket, Massachusetts: Procedures, data sources and analysis, National Oceanic and Atmospheric Administration, National Environmental Satellite, Data, and Information Service, National Geophysical Data Center, Marine Geology and Geophysics Division.
- Hakim, A. R., Cowles, G. W., and Churchill, J. H. (2013). The impact of tidal stream turbines on circulation and sediment transport in Muskeget Channel, MA. *Marine Technology Society Journal*, 47(4), 122-136. doi:10.4031/mts.j.47.4.14
- Johnson, K. S., and Petty, R. L. (1983). Determination of nitrate and nitrite in seawater by flow injection analysis. *Limnology and Oceanography*, 28, 1260 – 1266.
- Liu, C., Cowles, G. W., Churchill, J. H., and Stokesbury, K. D. (2015). Connectivity of the bay scallop (*Argopecten irradians*) in Buzzards Bay, Massachusetts, U.S.A. *Fisheries Oceanography*, 24(4), 364-382. doi:10.1111/fog.12114.
- Liu, C., Cowles, G. W., Zemeckis, D. R., Cadrin, S. X., and Dean, M. J. (in press) Validation of a hidden Markov model for the geolocation of Atlantic cod. *Canadian Journal of Fisheries and Aquatic Sciences*.
- NECOFS (2017) Northeast Coastal Ocean Forecasting System (NECOFS) Main Portal <http://fvcom.smast.umassd.edu/necofs/>. Accessed: 2017-05-20.
- NOS Ocean Data Portal (2016) (Last Accessed: 2017-04-20). URL <https://data.noaa.gov/dataset>
- Pawlowicz, R., Beardsley, B., Lentz, S. (2002). Classical tidal harmonic analysis including error estimates in MATLAB using T_TIDE, *Computers and Geosciences*, 28 (8), 929–937.
- Pruessner, A., Fanelli, P., Paternostro, C. (2007). C-MIST: An automated oceanographic data processing software suite. in: *Proceedings of the OCEANS 2007 Conference*.
- Sharp, J. H. (1974). Improved analysis for particulate organic carbon and nitrogen from seawater. *Limnology and Oceanography*, 19, 984-989.

- Signell, R. (1987). Tide and wind-forced currents in Buzzards Bay, Massachusetts, M.S. Thesis, Massachusetts Institute of Technology.
- Strickland, J. D. H., and Parsons, T. R. (1972). Determination of ammonia. *In* A Practical Handbook of Seawater Analysis, Fisheries Research Board of Canada, Bulletin 167 (Second Edition), 310 pages.
- Twomey, E.R. and Signell, R.P. (2013). Construction of a 3-arcsecond digital elevation model for the Gulf of Maine, U.S. Geological Survey Open-File Report 2011–1127, 24 pp, <https://pubs.usgs.gov/of/2011/1127/>.
- USACE, (2011). Cape Cod Canal Condition Survey, Tech. Rep. 11-1154, U.S. Army Corps of Engineers, New England District, Concord, MA.
- Williams, T., and Neill, C. (2014). Buzzards Bay Coalition Citizens' Water Quality Monitoring Program, "Baywatchers", 5 Year Quality Assurance Project Plan.
- Willmott, C. J. (1981). On the validation of models, *Physical Geography*, 2 (2), 184–194.

Tables and Figures

Table 1. Modeled discharge scenarios.

	Flow Rate (MGD)	TN Conc. (mg l ⁻¹)
Current MMA Discharge	0.03	100
Projected Minimum Flow Rate	3	3
Projected Maximum Flow Rate	10	3

Table 2. For four regions of particular interest, comparison of the averaged measured background concentration of TN with the projected additional TN concentration due a 10 MGD effluent discharge from the MMA outfall emerging into the canal with a TN concentration of 3 mg l⁻¹. See Figure 7 for areas over which the averages were taken.

	Measured Background*		Modeled Effluent Addition	
	µg l ⁻¹		µg l ⁻¹	
	Ave.	St. Dev	Ave.	St. Dev**
Buttermilk Bay	422	85	1.2	0.2
Butler Cove	555	92	1.4	0.4
Onset Bay	365	80	1.7	0.3
Cape Cod Bay	275	241	0.3	0.1

*The averaged background concentrations were computed from measurements taken over 2006-2016 at the locations shown in Figure 7.

**The standard deviation of the modeled values was computed from the hourly values of the spatial averages.

Table 3. Phase and amplitude of the observed and modeled M_2 tidal constituent at six tidal stations in upper Buzzards Bay and Cape Cod Canal. Columns 6 and 7 show the model skill in reproducing annual time series of tidal elevation at each site.

	M_2 Amp [m]		M_2 Phase [$^{\circ}G$]		Skill	
	<i>Obs</i>	<i>Model</i>	<i>Obs</i>	<i>Model</i>	<i>RMSE</i> [m]	<i>Willmott</i> [-]
Piney Point	0.58	0.54	6.94	6.85	0.053	0.98
Railroad Bridge	0.52	0.47	49.91	58.47	0.079	0.96
Canal East	1.28	1.25	108.36	106.44	0.046	1.00
Sagamore	1.11	1.08	107.30	103.43	0.062	0.99
Great Hill	0.56	0.54	10.70	7.03	0.068	0.97
Nyes Neck	0.54	0.53	8.00	4.67	0.034	0.99

Table 4. Skill assessment for the velocity computed from an annual time series constructed using the major axis of the constituents of the vertically averaged velocity field at 5 CMIST stations within the model domain (see Figure 10 for locations).

CMIST Station No.	Location	Willmott [-]	RMSE [ms^{-1}]	Mean observed [ms^{-1}]	Mean modeled [ms^{-1}]
COD0901	Cape Cod Canal, East End	0.99	0.09	0.97	0.97
COD0902	Cape Cod Canal, Sagamore Bridge	0.98	0.18	1.05	1.17
COD0903	Cape Cod Canal, Bournedale	0.96	0.25	1.03	1.22
COD0905	Hog Neck	0.99	0.10	0.96	0.92
COD0906	Abiels Ledge	0.99	0.05	0.46	0.44



Figure 1. Satellite image of the Massachusetts Maritime Academy (MMA) facility with the MMA outfall marked by a blue cross.

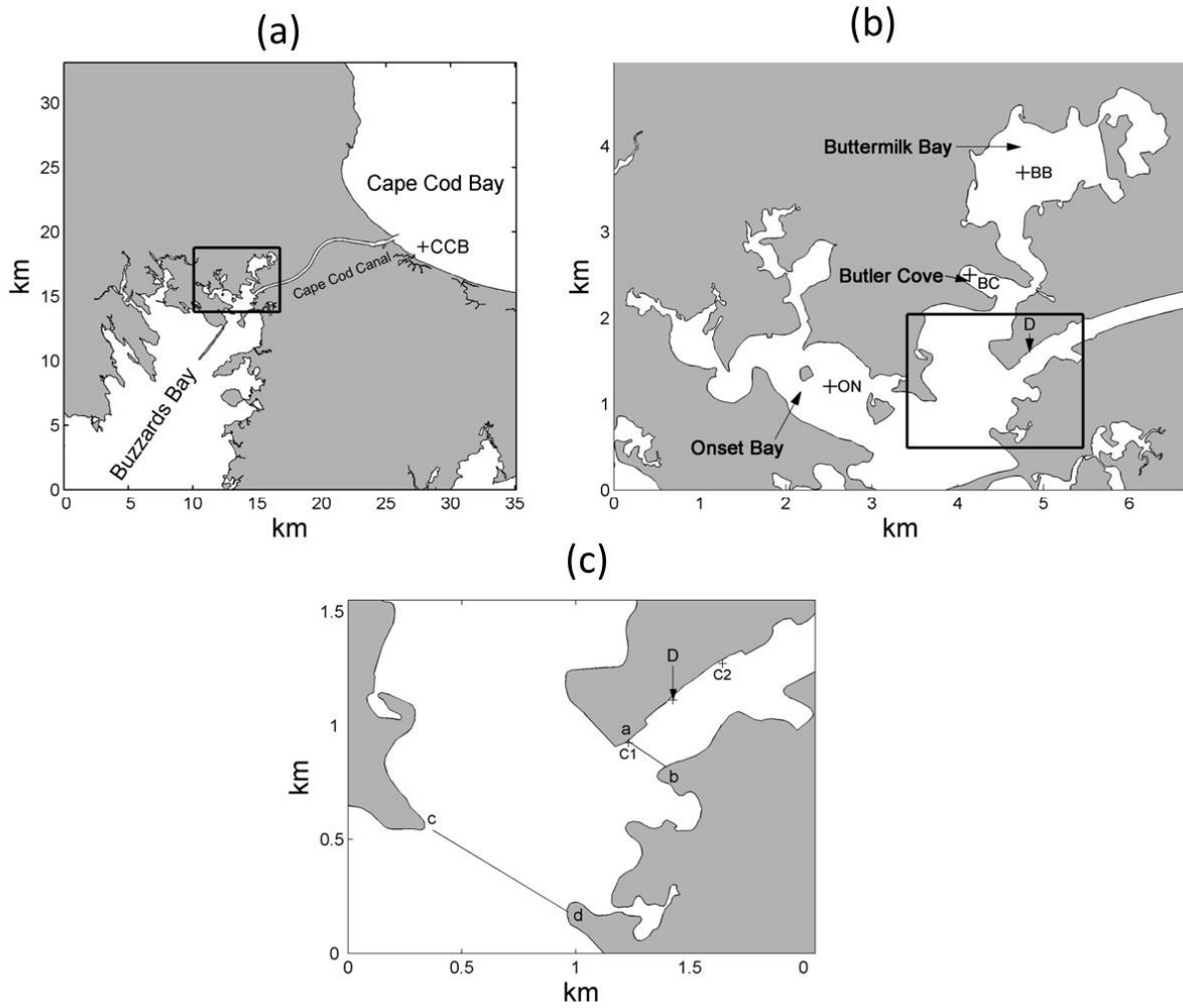


Figure 2. Nested view of the region of study. Indicated are areas of particular concern: Butler Cove, Cape Cod Bay, Onset Bay and Buttermilk Bay. Also shown are points (sites CCB, ON, BC, BB, C1 and C2) and transects [lines a-b and c-d in panel (c)] for which model data will be shown in subsequent figures. The discharge location is marked in (b) and (c) by an arrow labeled 'D'.

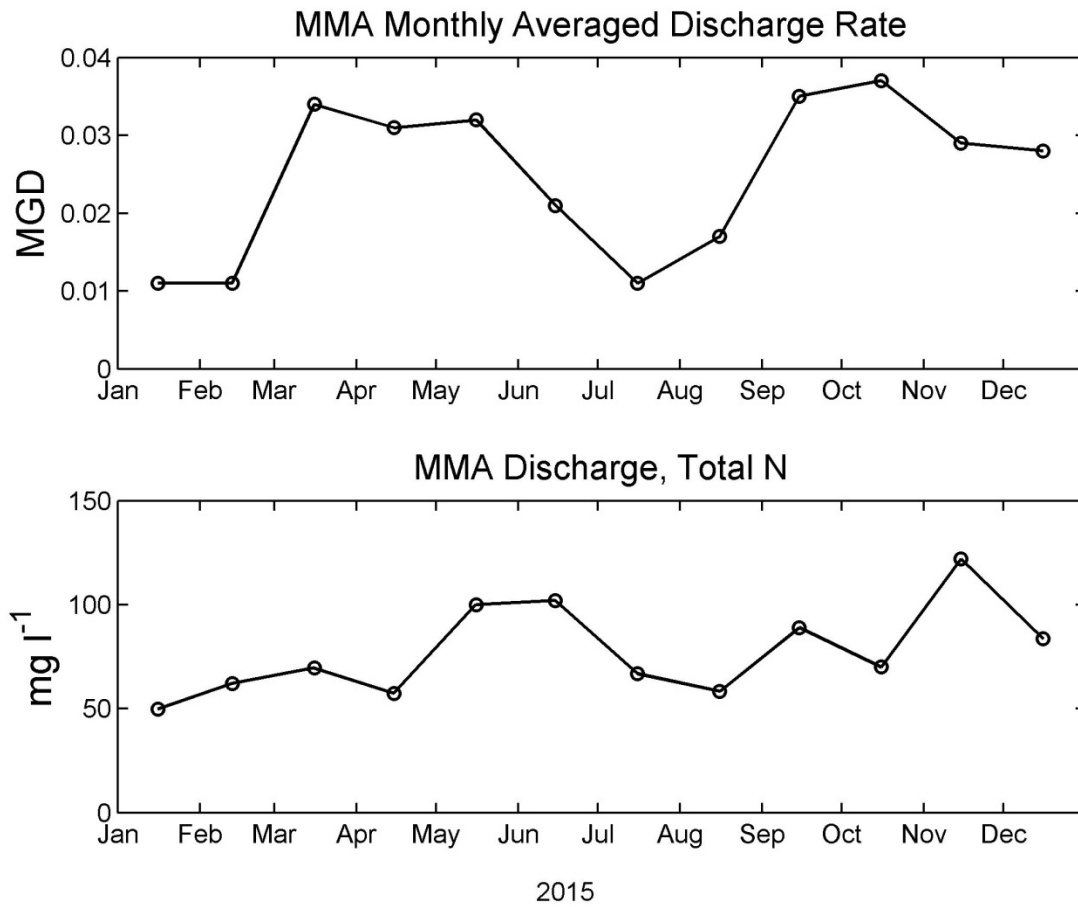


Figure 3. Monthly averaged volume discharge rate (top panel) and total N concentration (bottom panel) in the effluent discharged from the MMA waste water treatment facility in 2015.

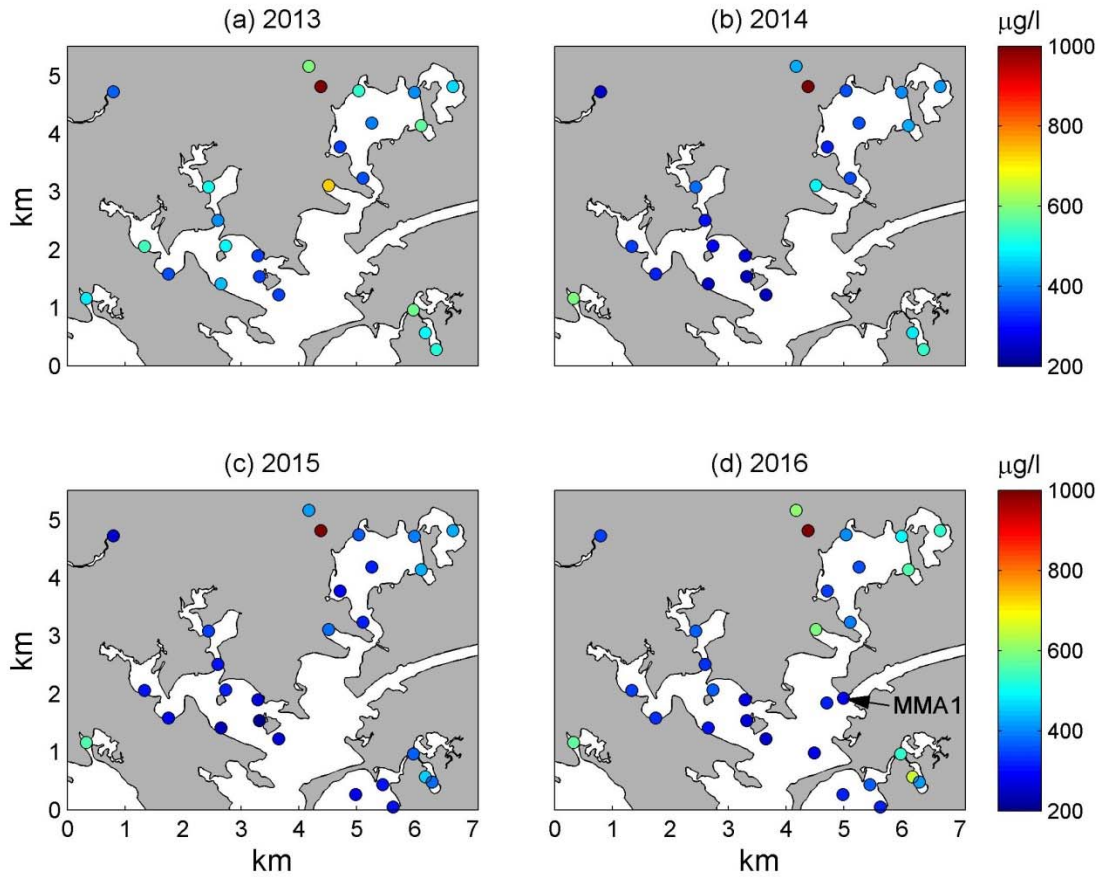


Figure 4. Scatter plots of yearly averaged TN concentration in ($\mu\text{g l}^{-1}$) in upper Buzzards Bay, determined using TN concentrations from the Buzzards Bay Coalition's long-term citizen-science monitoring program (see text). The site labeled 'MMA1' in (d) is the program's sampling location closest to the MMA sewage discharge.

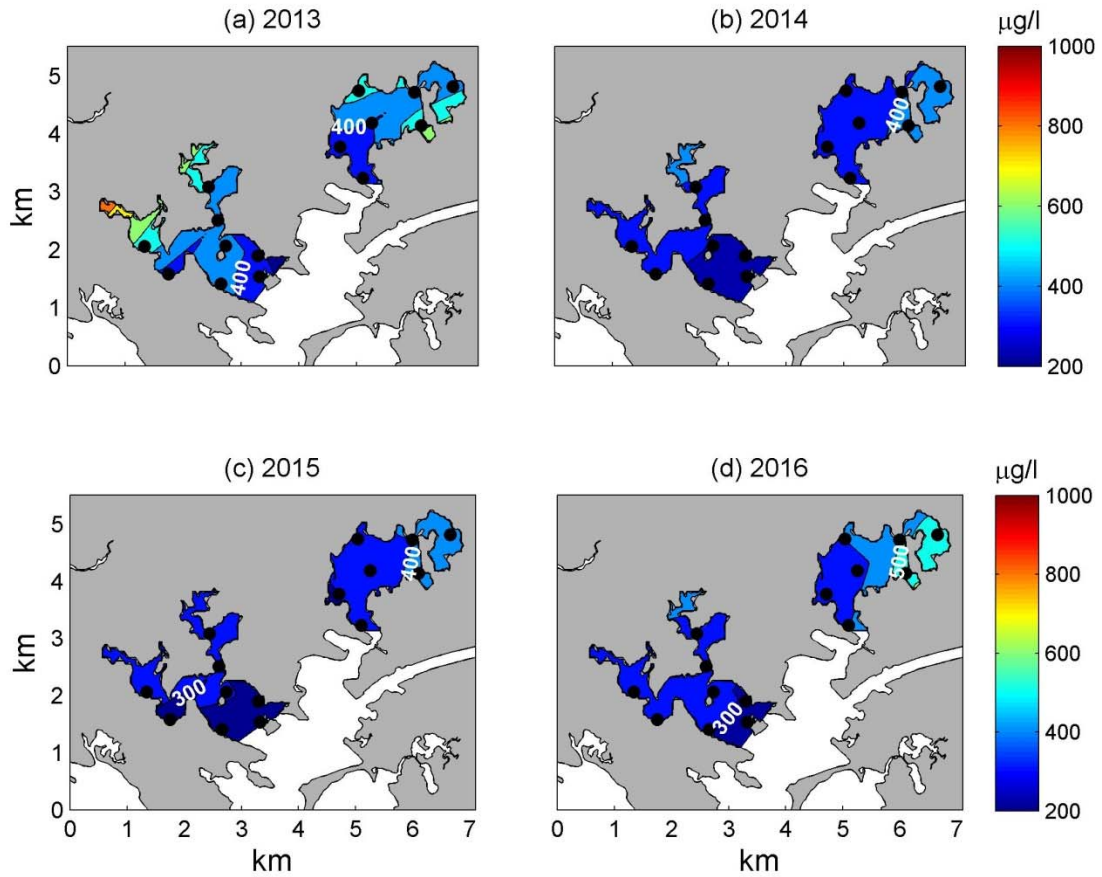


Figure 5. Contours of yearly averaged TN concentration in ($\mu\text{g l}^{-1}$) in Buttermilk and Onset Bays, determined using TN concentrations from the Buzzards Bay Coalition's long-term citizen-science monitoring program (see text). The contours were determined with a two-dimensional linear interpolation algorithm using averaged concentrations from the stations marked by black dots.

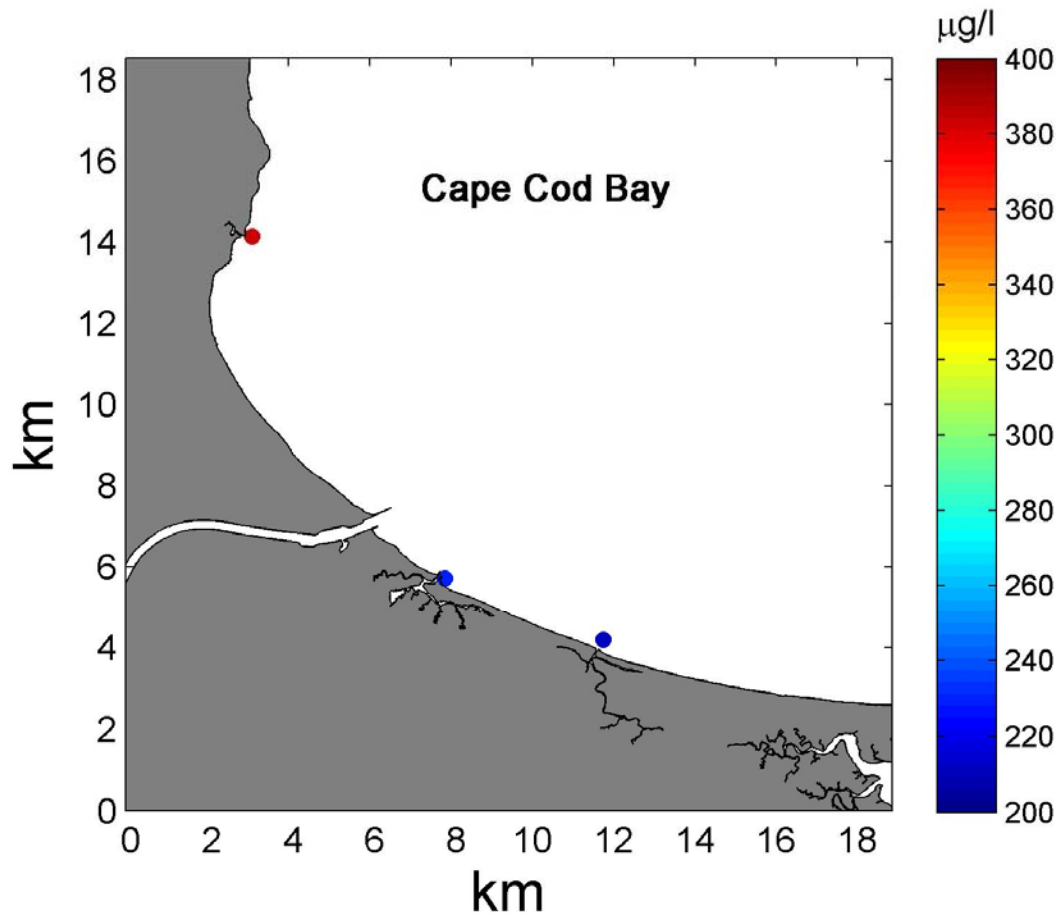


Figure 6. Scatter plot of averaged TN concentration in ($\mu\text{g l}^{-1}$) in Cape Cod Bay, determined using TN concentrations compiled by the Center for Coastal Studies (see text). The averaging period extended over the full data set from each location (2006-2016 for the northernmost station, 2006-2010 for the southern two stations).

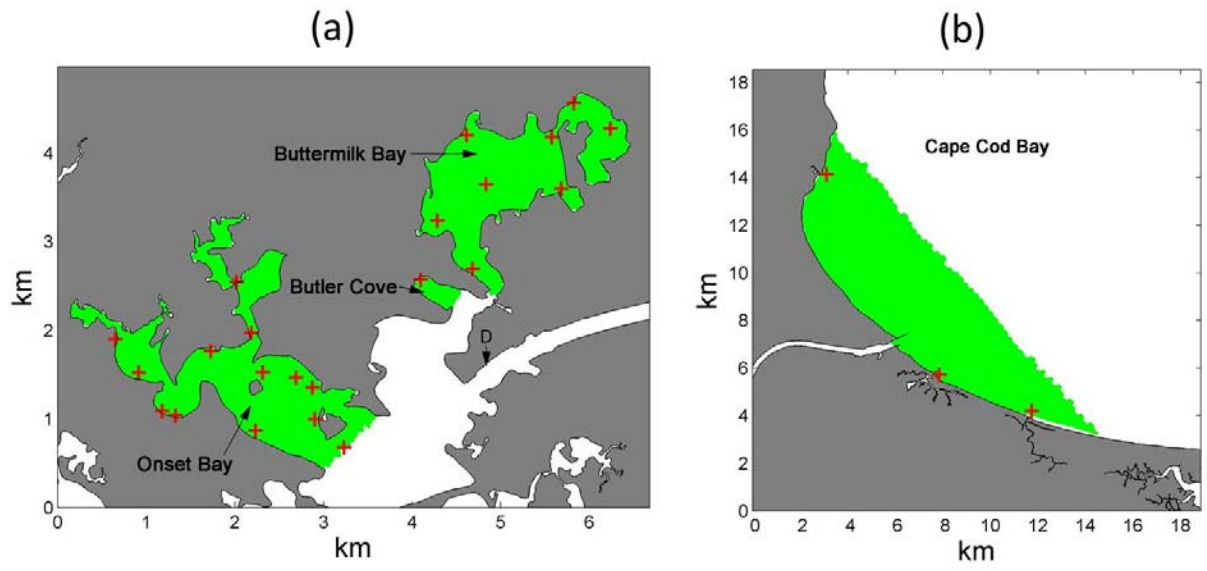


Figure 7. Areas over which measured (at red points) and modeled (green shading) TN concentrations were averaged.

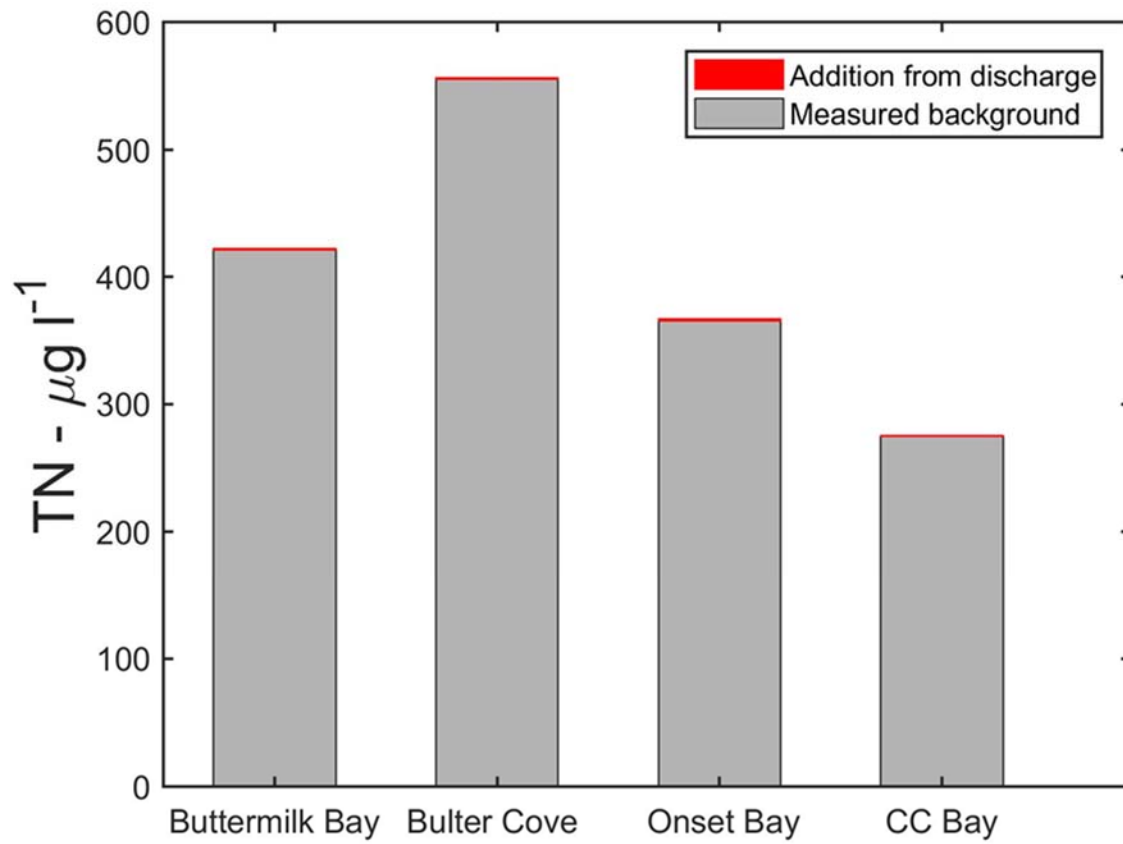


Figure 8. Comparison of averaged measured TN concentration in areas of interest with the modeled added TN concentration from an effluent discharge of 10 MGD. See Figure 7 for averaging areas and Table 2 for concentration values.

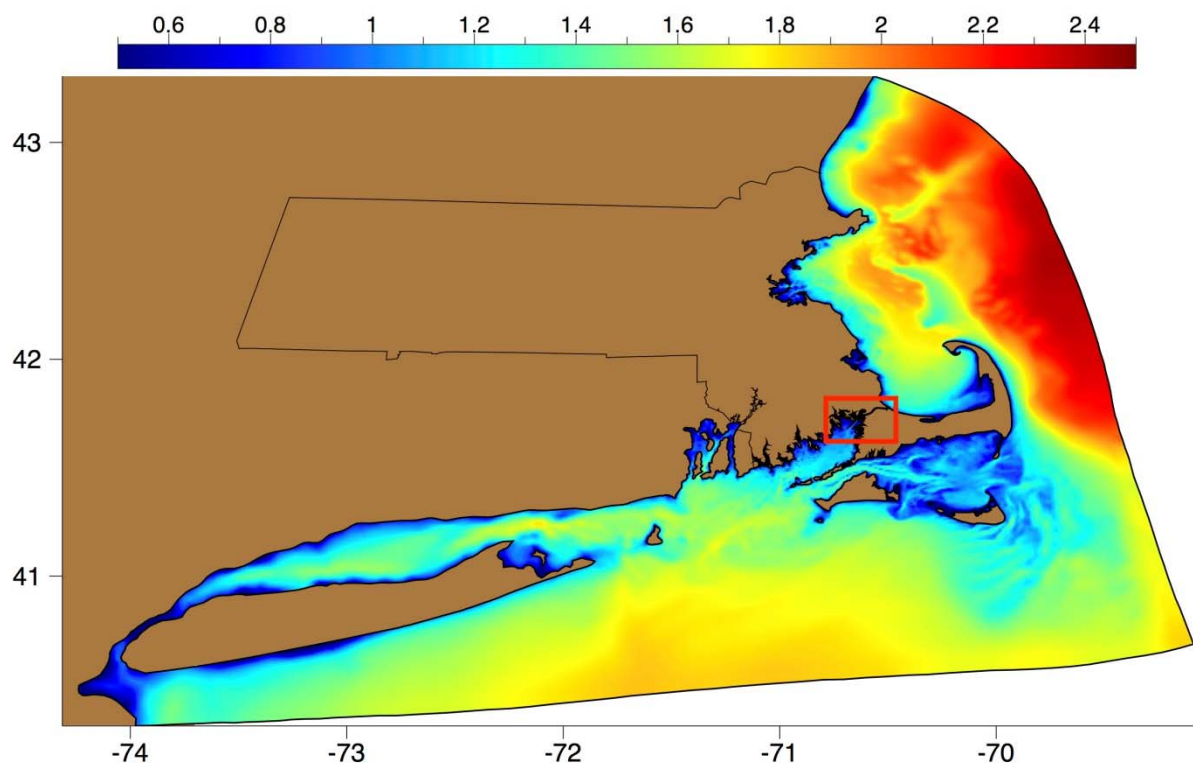


Figure 9. SEMASS-FVCOM model domain and bathymetry [$\log_{10}(\text{m})$].

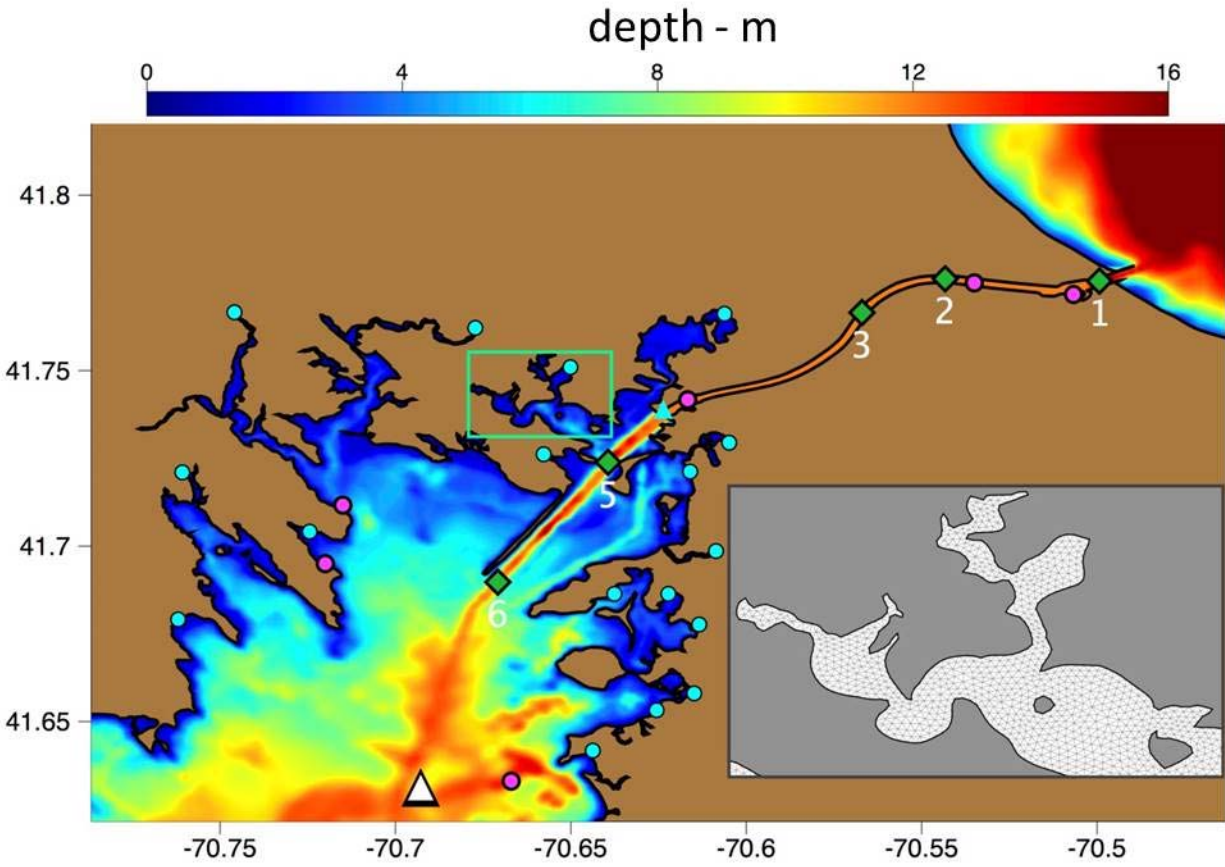


Figure 10. Portion of the FVCOM-SEMASS domain in upper Buzzards Bay with bathymetry (m) (see Figure 9 for the full model domain). Also shown are measurement locations for CMIST upward-looking ADCP (numbered green diamonds), tidal harmonic elevation stations (magenta circles), and Mass Division of Marine Fisheries long-term bottom temperature record (white triangle) as well as the locations for point sources of freshwater input to the upper bay (cyan circles) and approximate location of the proposed outfall (cyan triangle). CMIST ADCPs are numbered East to West. Lower Figure Inset: Model grid in Onset Bay.

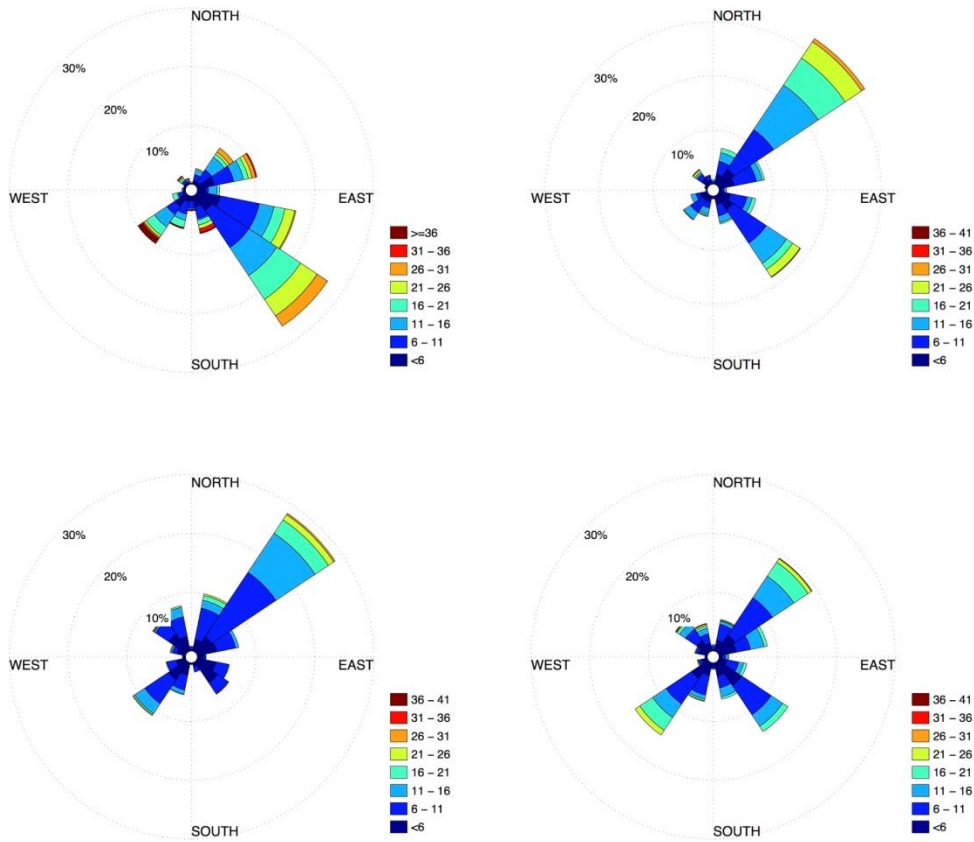


Figure 11. Graphic representation of wind statistics of the modeled surface wind forcing at the location of the proposed outfall. Magnitude is in knots. Upper Left: Jan 1 - Mar 31, 2015. Upper Right: Apr 1 - June 30, 2015. Lower Left: Jul 1 - Sep 30, 2015. Lower Right: Oct 1 - Dec 31, 2015.

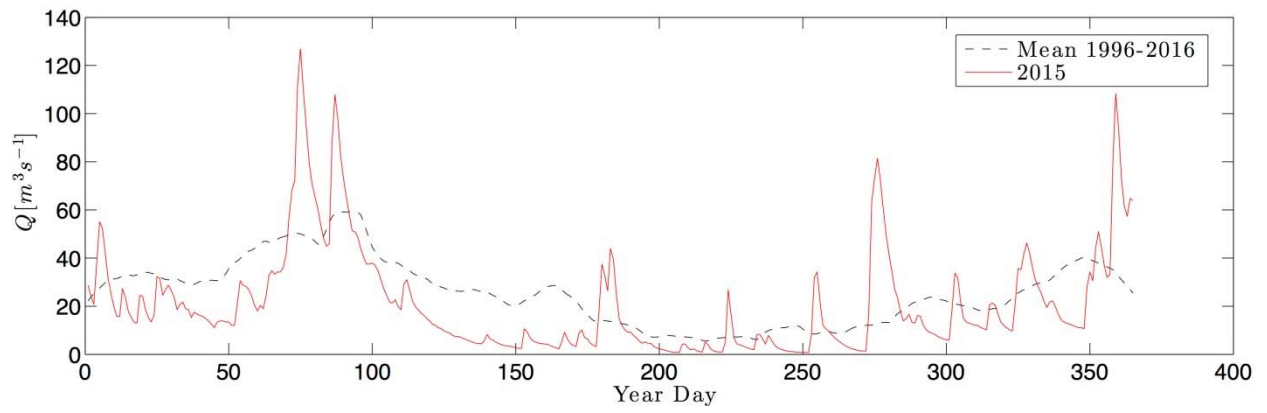


Figure 12. Total discharge ($m^3 s^{-1}$) from all freshwater point sources to Buzzards Bay by year day.

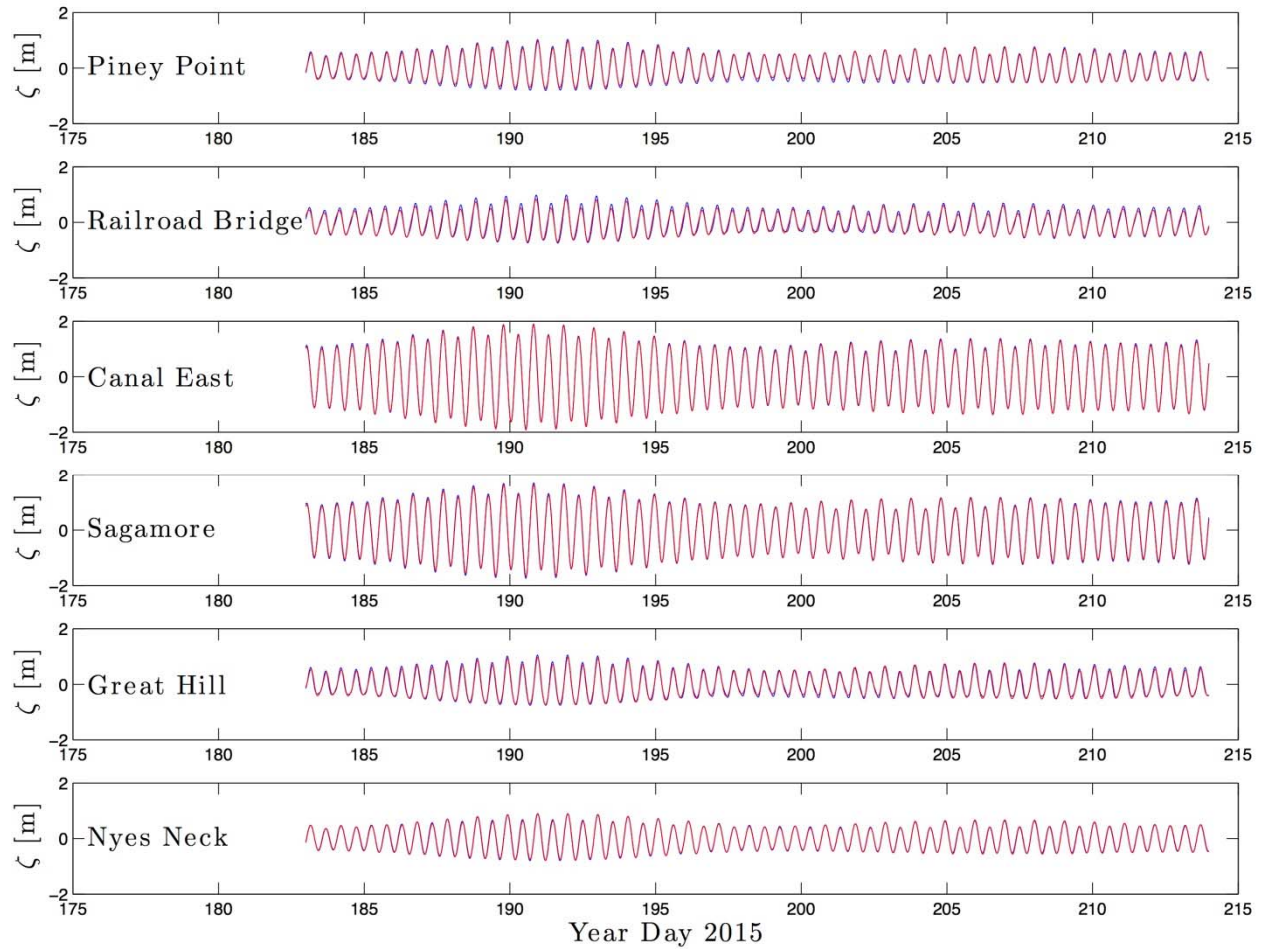


Figure 13. Comparison of time series of tidal surface elevation [m] from measurements (blue) and modeled (red) at the six NOS tidal stations in upper Buzzards Bay and Cape Cod Canal (Figure 10) during July 2015. The model-produced series is overlain over the observations and is often the only visible series above.

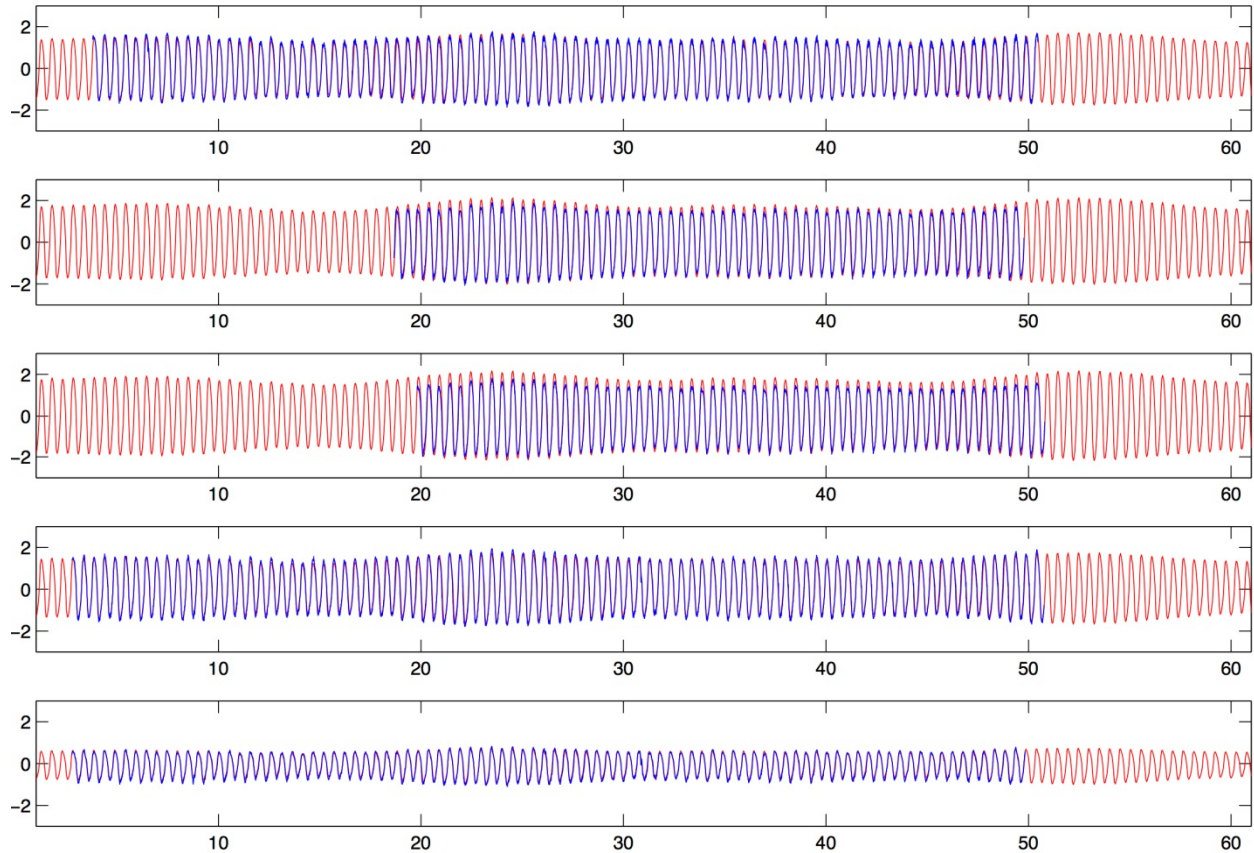


Figure 14. Comparison of time series of depth-averaged velocities (m s^{-1}) for the CMIST period (June-July, 2009). Time is days since June 1, 2009. The red line is the model-computed value and the blue line is the observed. The comparisons for CMIST Stations 1,2,3,5,6 (see Figure 10 for locations) are arranged from top to bottom. Note that the observations cover different time periods. Model results are shown for the first 61 days of 2009 and fully encompass each measured series.

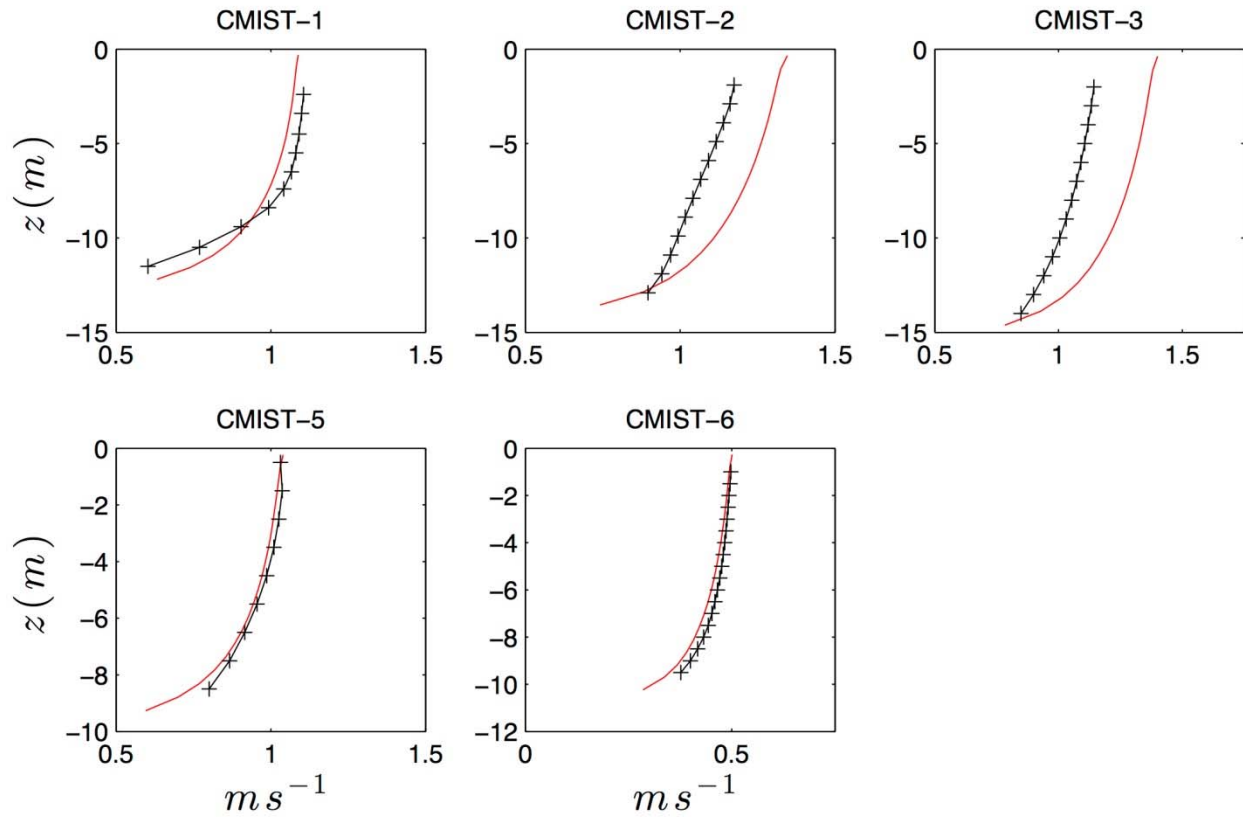


Figure 15. Profiles of modeled (red solid lines) and observed (black lines with + symbols) annual mean velocity magnitude at CMIST ADCP locations (Figure 10).

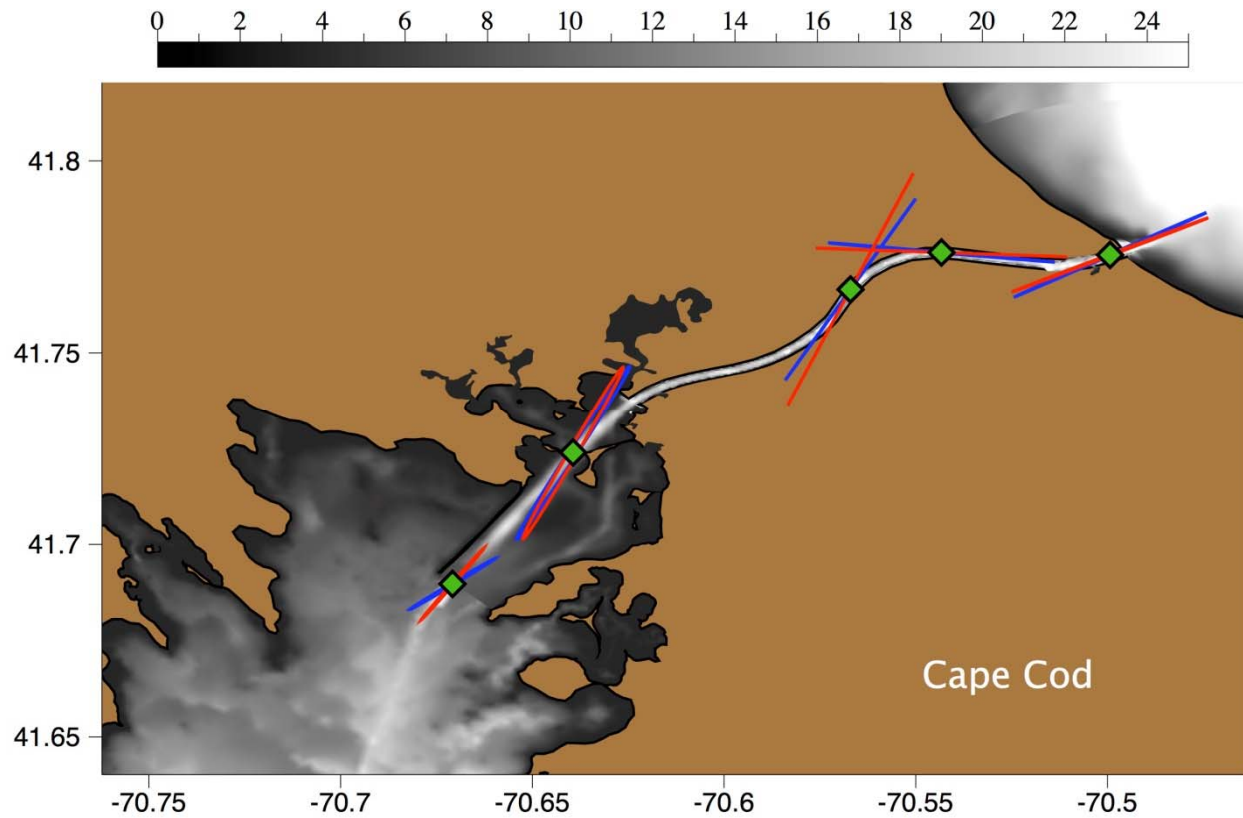


Figure 16. Tidal ellipses of model-computed (red) and observed (blue) depth-averaged velocity at CMIST stations in upper Buzzards Bay. Shading represents bathymetry (m).

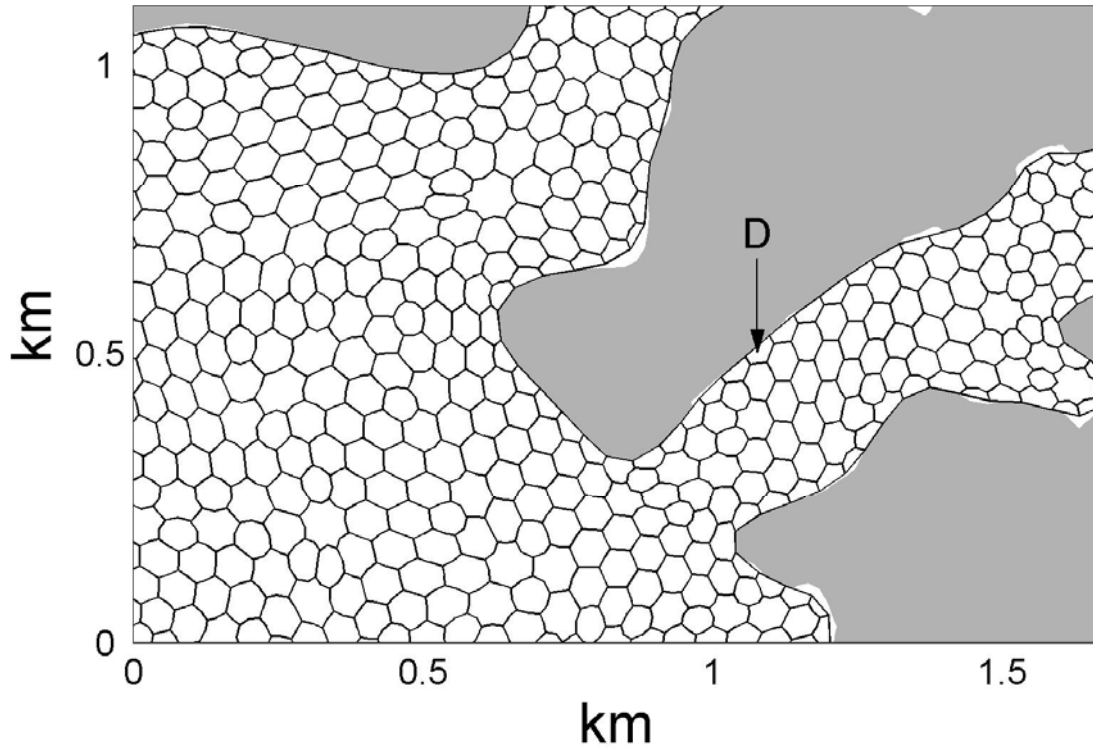


Figure 17. Borders of the tracer control volumes of the model grid in the area of the MMA discharge outfall (labeled 'D' above). The control volume containing the outfall measures roughly 50 by 30 m.

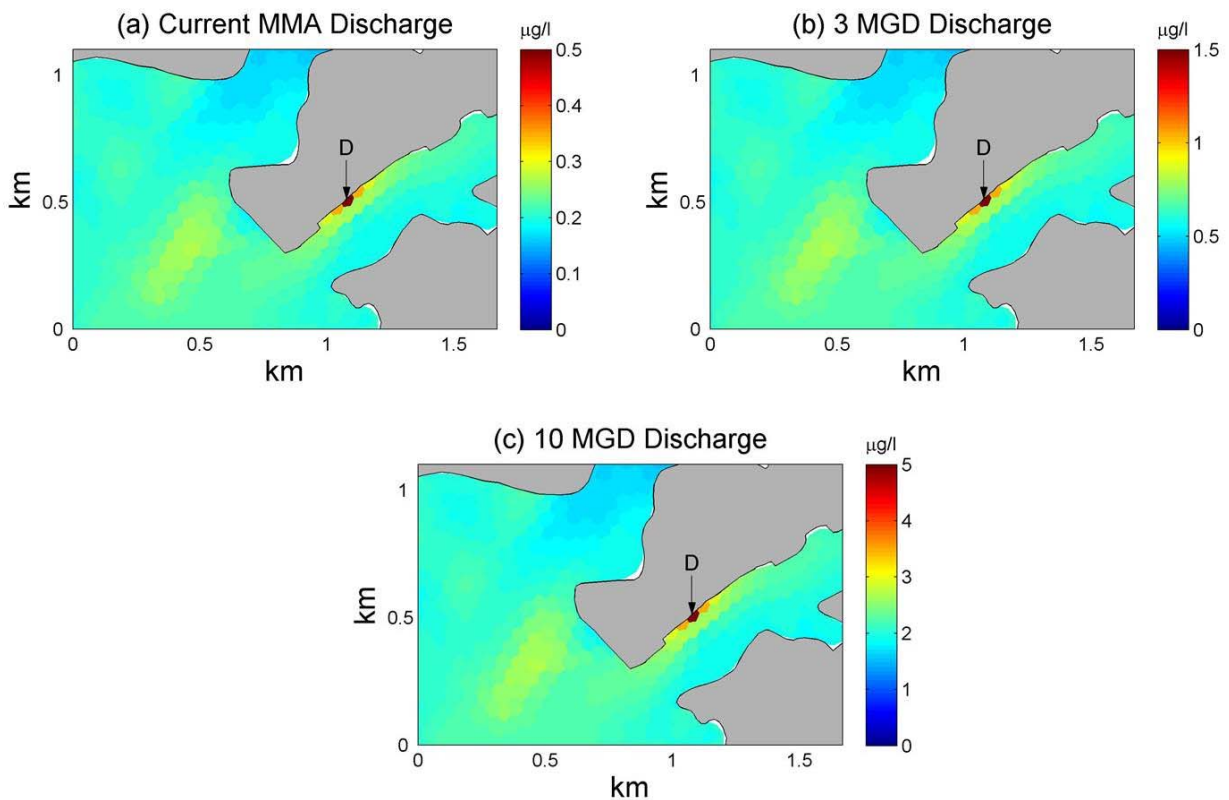


Figure 18. Vertically and temporally averaged concentrations ($\mu\text{g l}^{-1}$) of total nitrogen (TN) contained in the discharged effluent (not including the background TN concentrations) for three discharge scenarios (Table 1). The fields were computed from the model fields of July 2015. Note that different color scales are used for each panel. Note also that the maximum concentration in each panel [e.g., $7 \mu\text{g l}^{-1}$ in panel (c), which is slightly larger than the scale maximum to more clearly show the spatial variations of the TN field] is far lower than the background TN concentrations shown in Figures 4-5 (which are $200\text{-}800 \mu\text{g l}^{-1}$).

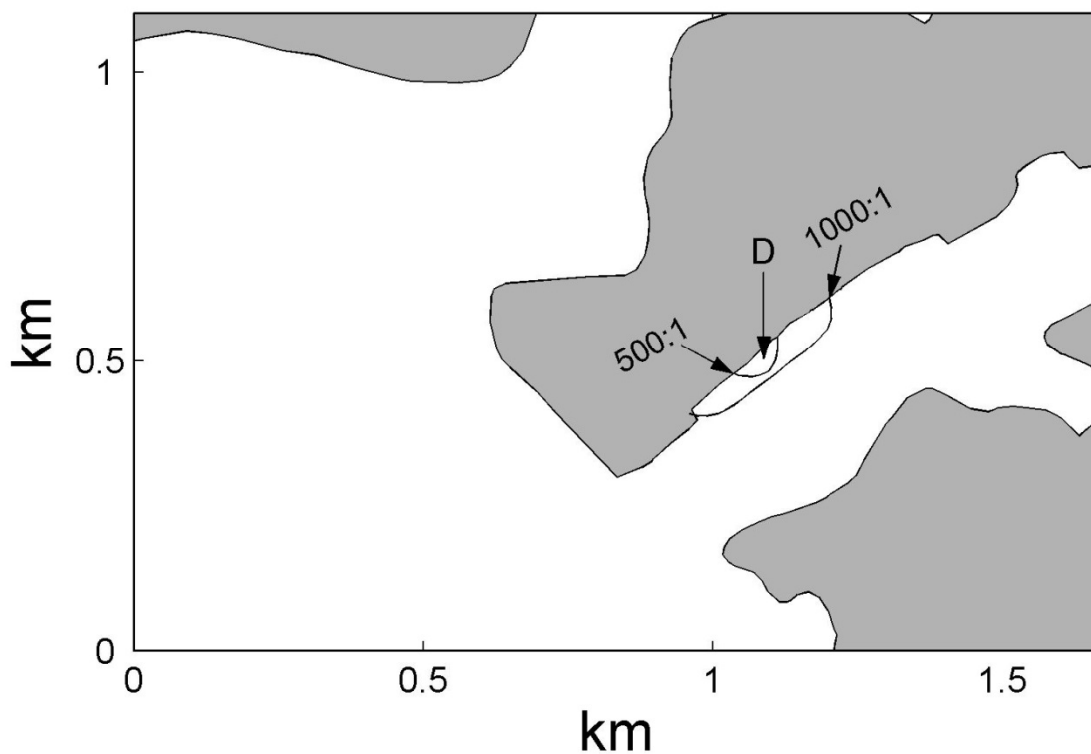


Figure 19. Contours of 500:1 and 1000:1 dilution ratios (ratios of discharged concentration to vertically averaged modeled concentration) for a 10 MGD discharge. The field was determined from modeled concentrations of July 2015 (month with the largest area encompassed by the 1000:1 dilution ratio contour). The area encompassed by the 1000:1 contour above is approximately 0.13 km².

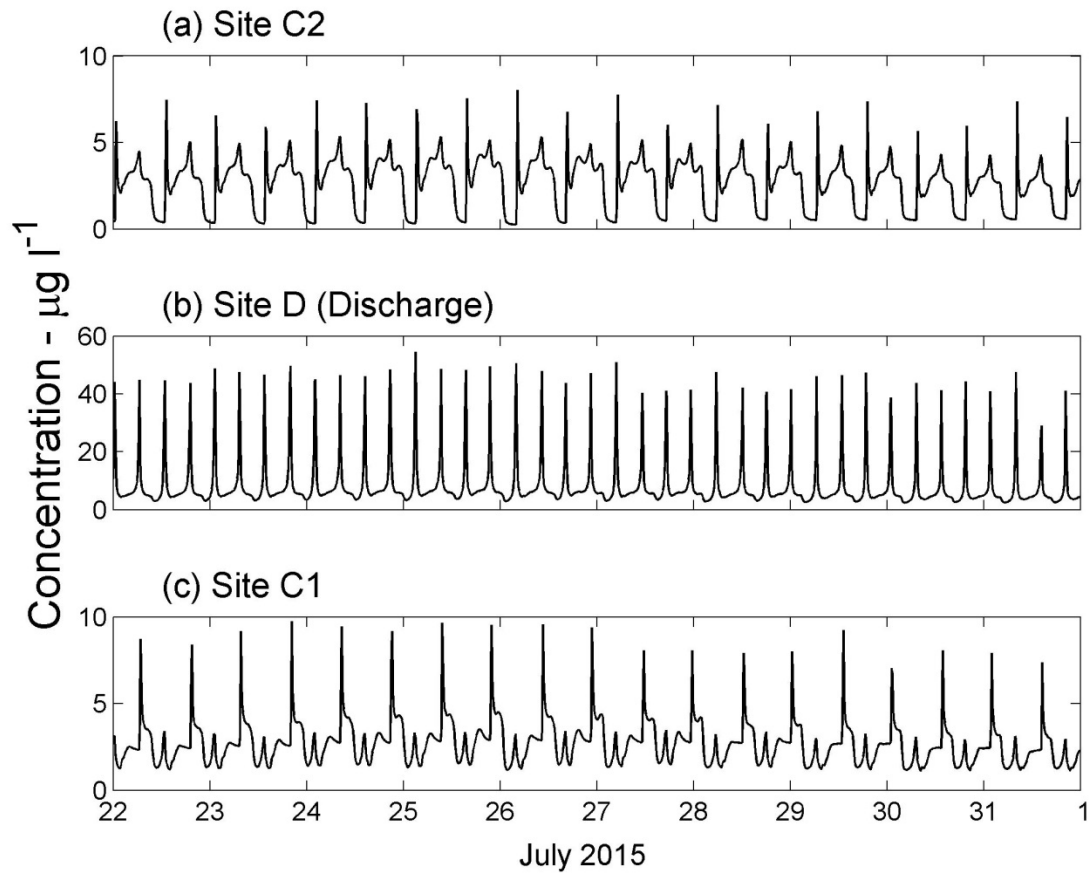


Figure 20. Modeled vertically averaged effluent TN concentrations ($\mu\text{g l}^{-1}$) at three sites near the western canal entrance (shown in Figure 3c) during late July (month with the highest near-discharge effluent TN concentrations). The fields were computed for a 10 MGD discharge.

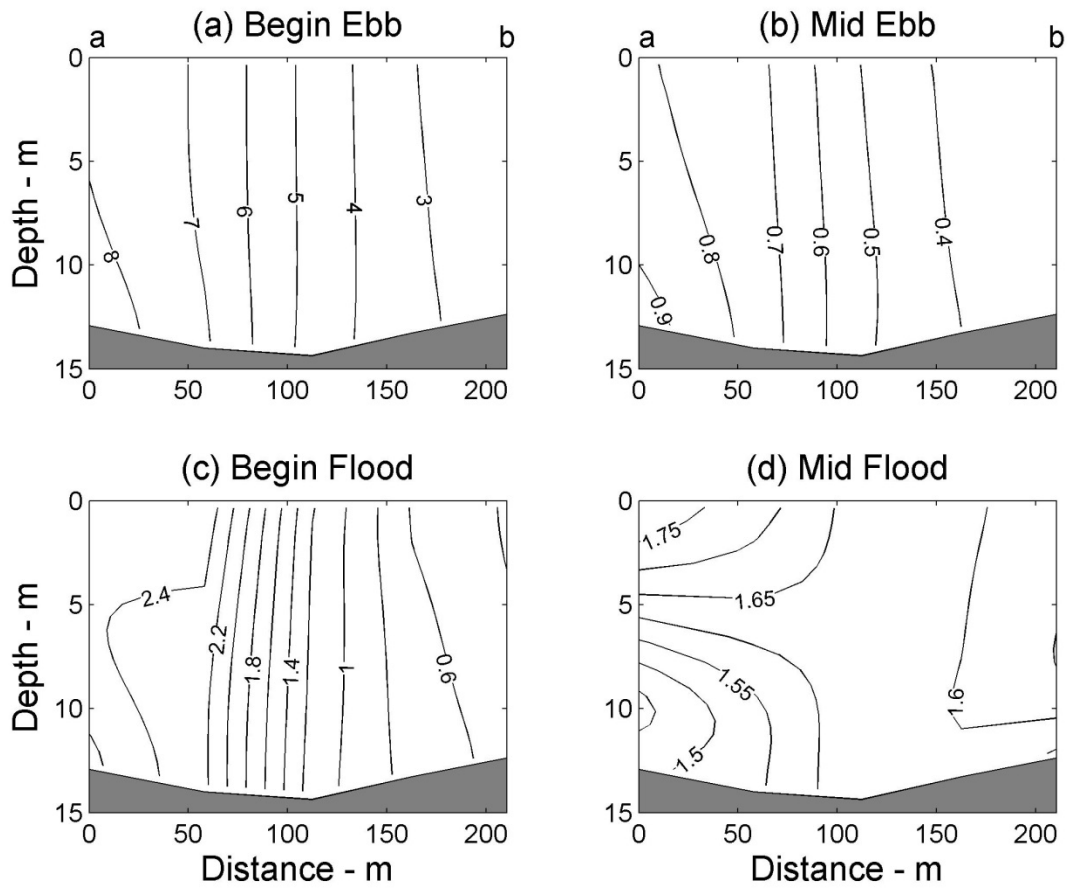


Figure 21. Representative modeled concentration fields of effluent TN ($\mu\text{g l}^{-1}$) at the western entrance to Cape Cod Canal (along line a-b in Figure 3c) for four phases of the tide. The fields were created with data from the tidal cycle with the maximum concentrations at the western canal entrance during August, and were computed for a 10 MGD discharge.

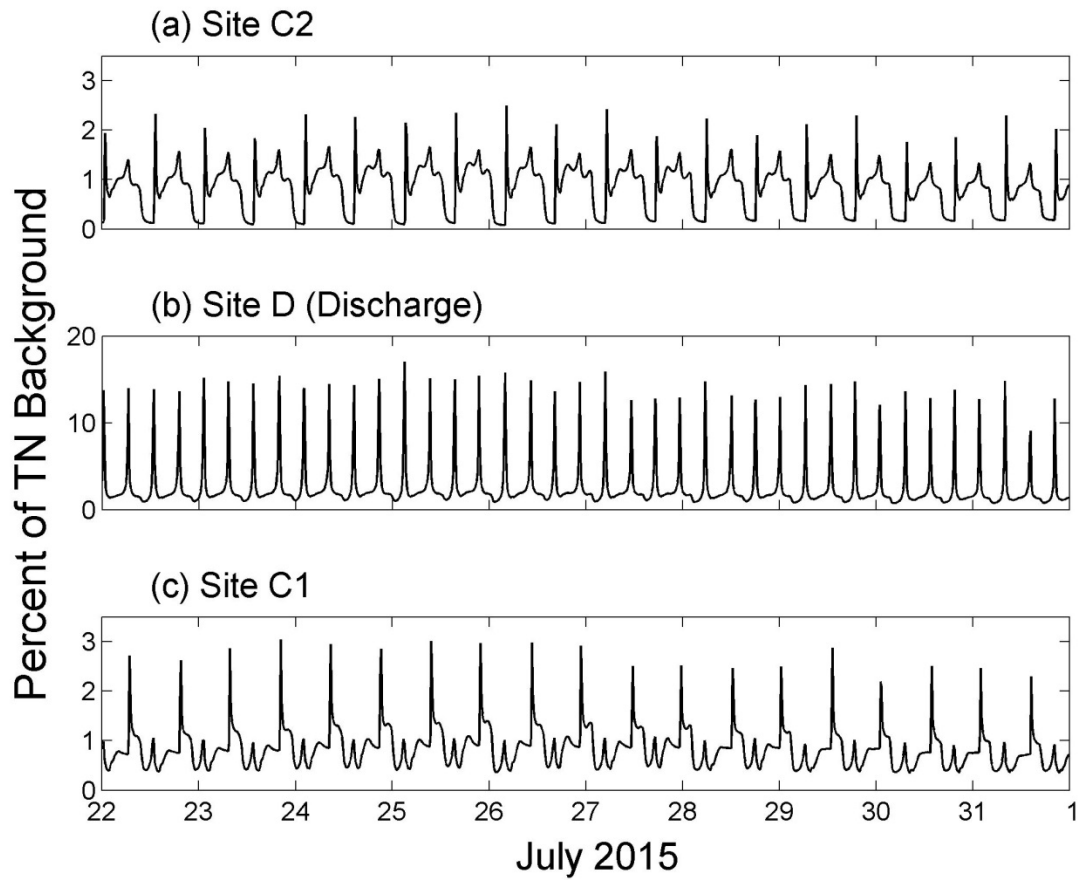


Figure 22. Same as Figure 20 except showing modeled vertically averaged effluent TN concentrations at three sites near the western canal entrance (shown in Figure 3c) as a function of the percent of the background TN concentration ($321 \mu\text{g l}^{-1}$) at the western entrance.

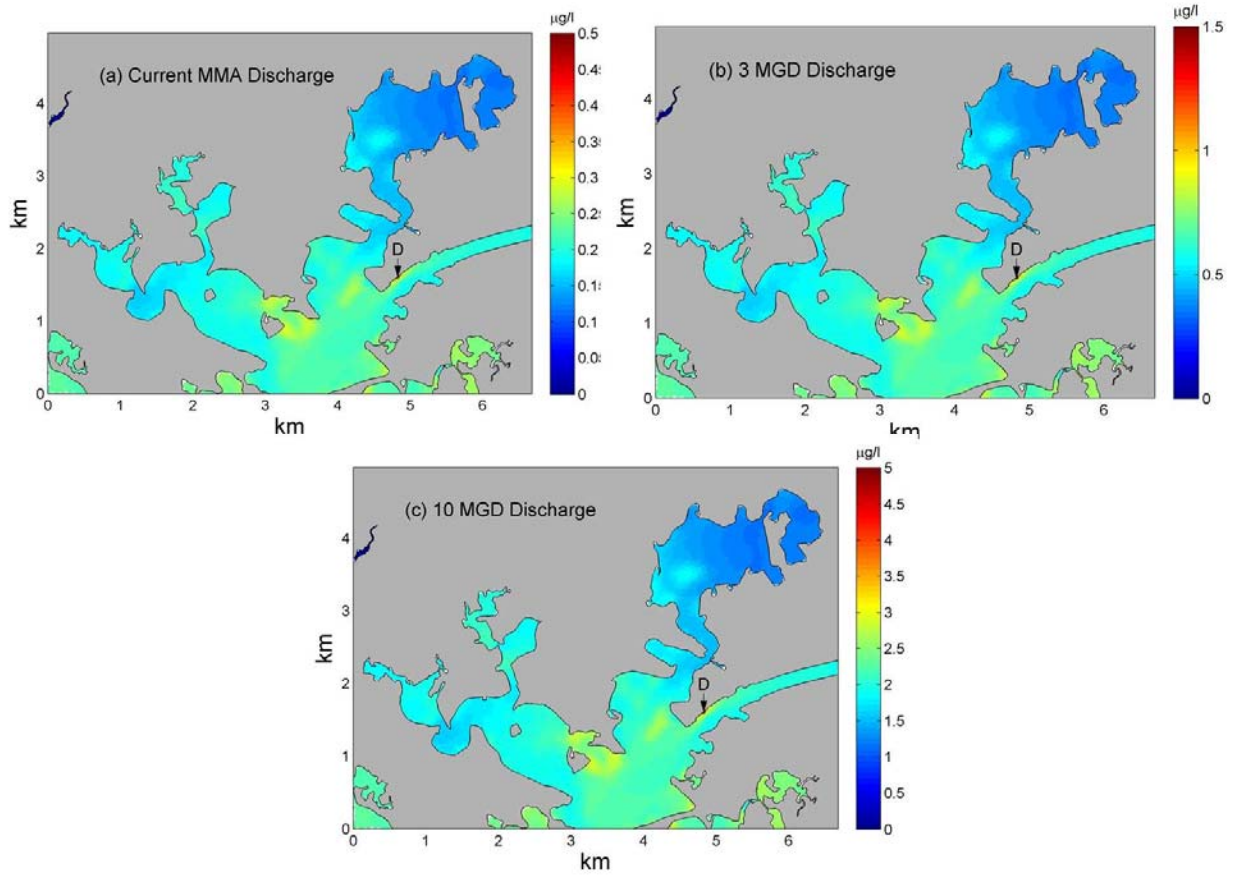


Figure 23. Same as Figure 18 except showing a larger-scale views of vertically averaged concentrations ($\mu\text{g l}^{-1}$) of effluent TN for three discharge scenarios (Table 1). Note again, the difference in scale in each panel and that the maximum concentration in each panel is far lower than the background TN concentrations shown in Figures 4-5.

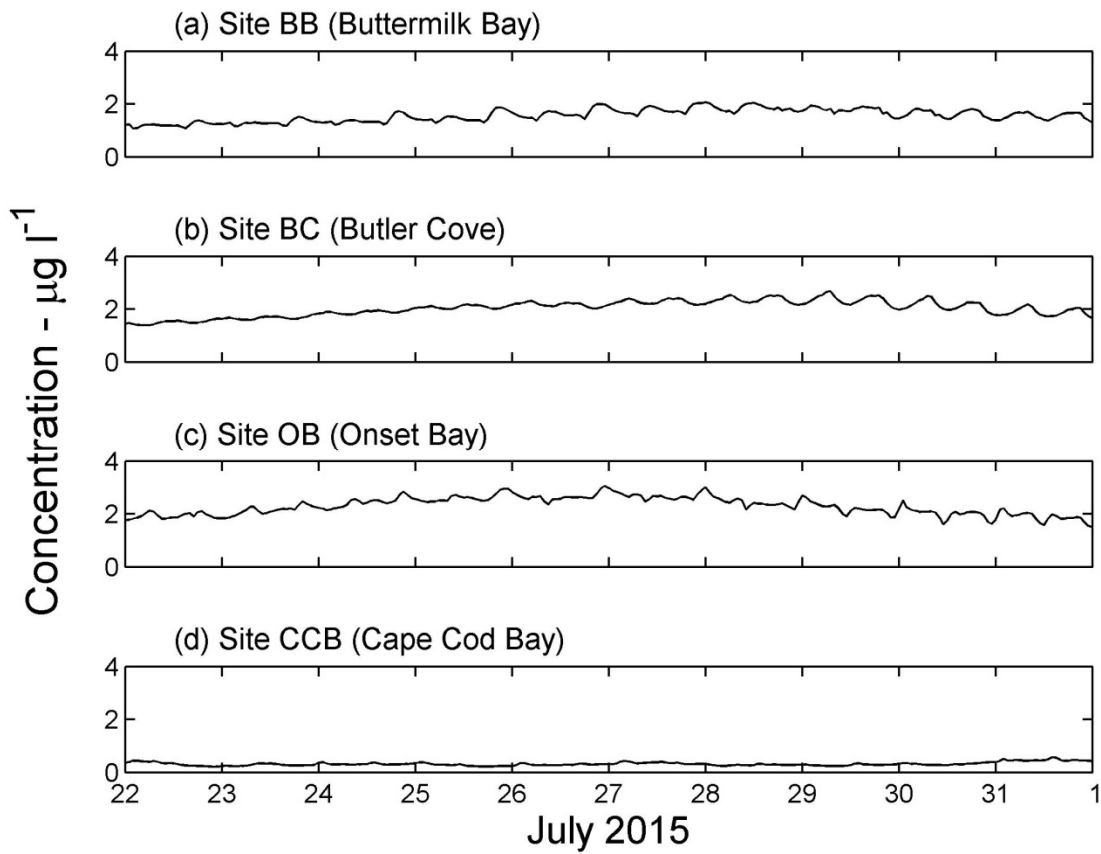


Figure 24. Modeled vertically averaged effluent TN concentrations (for a 10 MGD discharge) at sites in Cape Cod Bay and in Upper Buzzards Bay (shown in Figure 3a,b) during late July.

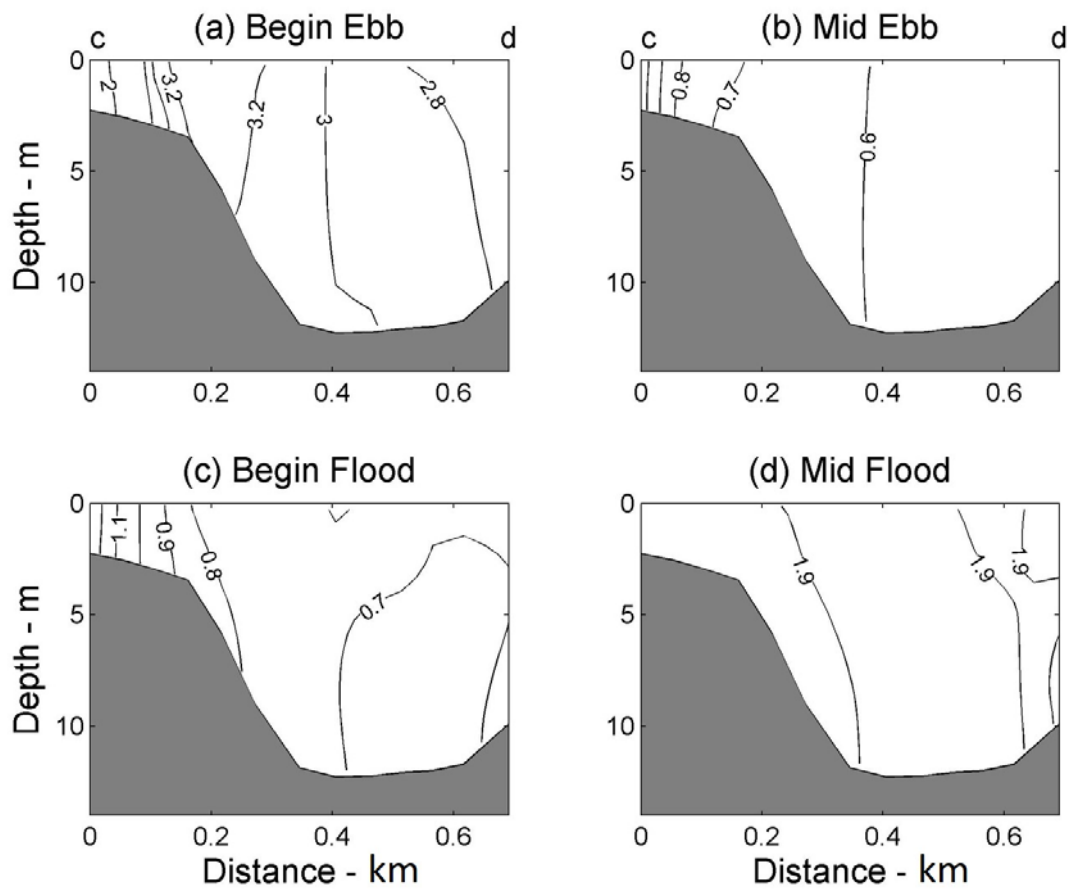


Figure 25. Same as Figure 21, except showing TN concentration fields ($\mu\text{g/l}$) in upper Buzzards Bay (along line c-d in Figure 3c).

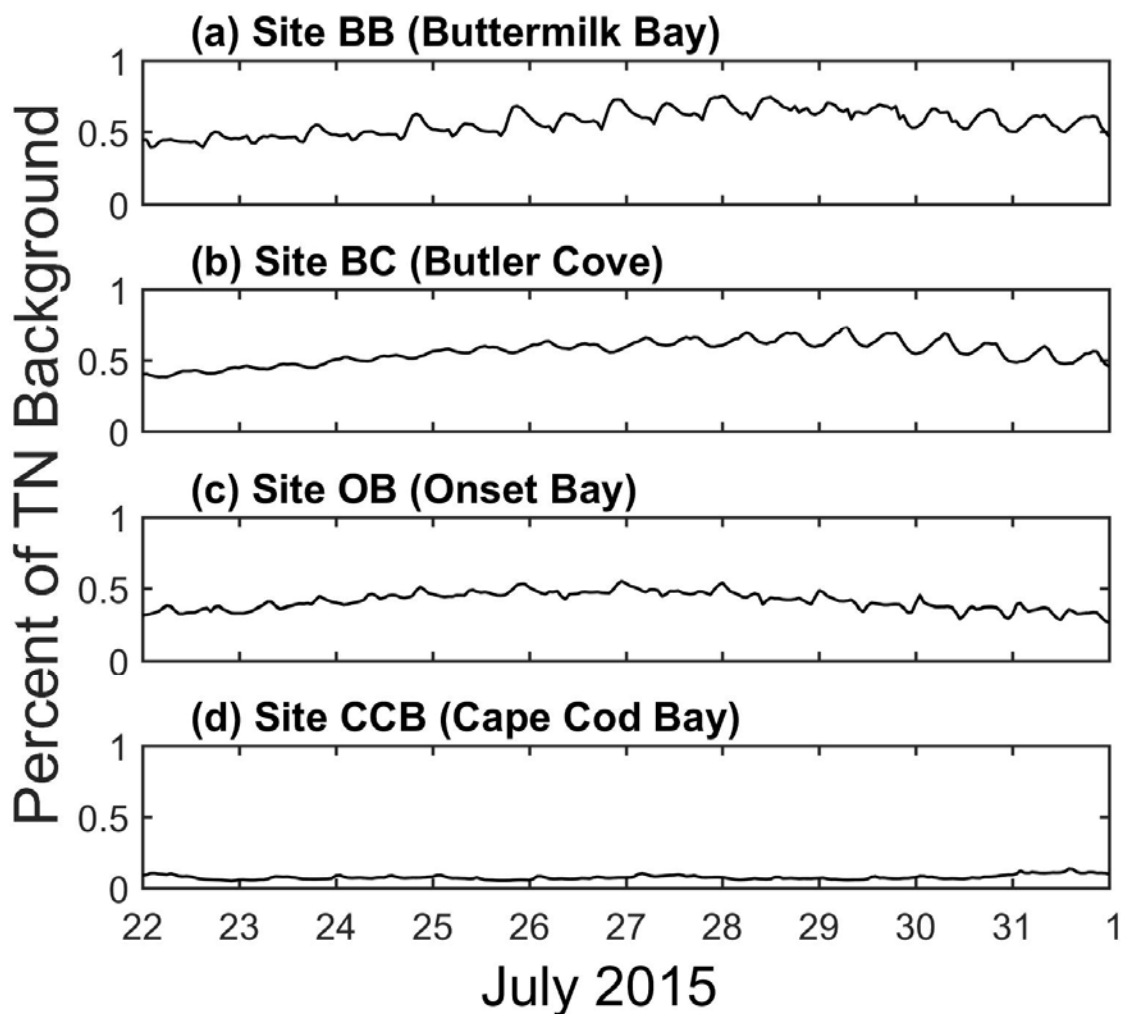


Figure 26. Same as Figure 24 except showing the effluent TN concentrations at points in each designated area (shown in Figure 3a,b) as a function of the percent of the measured TN background concentration in each area (Figure 8 and Table 2).

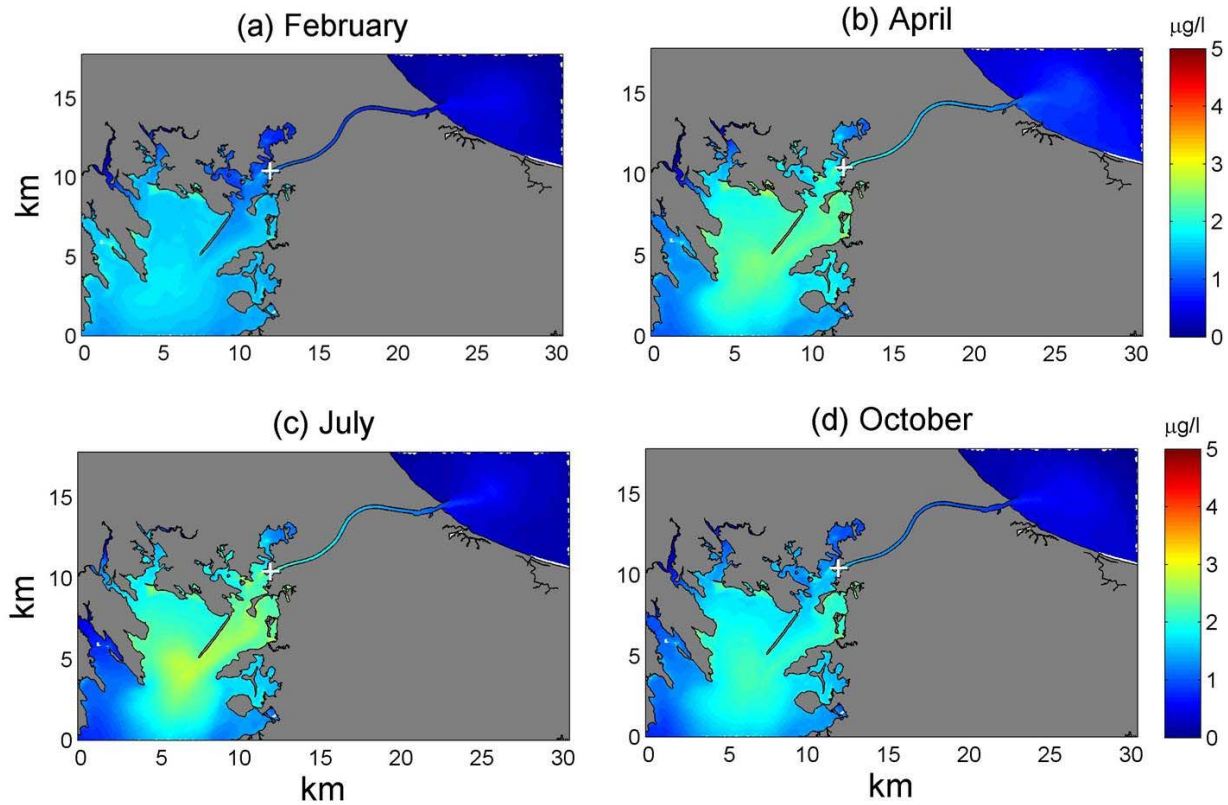


Figure 27. Modeled vertically averaged concentration fields (10 MGD discharge) of effluent TN ($\mu\text{g l}^{-1}$) for four months. The discharge location is marked with a white '+'. Apparent is a seasonal variation in the concentration fields. During winter and autumn (a and d), energetic currents driven by predominantly down-bay winds (Figure 11) produce maximum flushing of discharged effluent from Buzzards Bay, resulting in relatively low effluent TN concentrations in the upper bay. By contrast, modeled effluent TN concentrations in upper Buzzards Bay are somewhat higher (though still two orders of magnitude lower than ambient/existing conditions) during spring and summer (b and c), when wind forcing tends to be directed up the bay (Figure 11).

Appendix: Estimating the Volume Transport through Cape Cod Canal on a Single Tide

To roughly estimate the volume of water transported through the canal on a given flood or ebb tide, we may assume that the instantaneous volume flux, F , passing through a canal cross-section at a given time, t , is approximated by the product of the cross-section's area, A , and representative velocity, $u(t)$, flowing through the cross-section. This may be expressed as:

$$F(t) = Au(t).$$

Further, assuming that A is a product of a representative canal width, L , and depth, D (ignoring changes in D due to tidal excursions), gives:

$$F(t) = LDu(t).$$

As a first approximation, we may assume that flow through the canal is dominated by the semidiurnal tide with a period, P , of 12 hour 25 minutes, with $u(t)$ expressed as:

$$u(t) = U_a \sin\left(\frac{2\pi t}{P}\right),$$

where U_a is the peak tidal velocity. The instantaneous volume flux is then:

$$F(t) = LDU_a \sin\left(\frac{2\pi t}{P}\right).$$

The total volume of water, V , transported through the canal on a given flood or ebb tide is then the integral of the above over $\frac{1}{2}$ the tidal period, i.e.

$$V = LDU_a \int_0^{P/2} \sin\left(\frac{2\pi t}{P}\right) dt,$$

which easily solves to:

$$V = \frac{PLDU_a}{\pi}.$$

To estimate V in the area of MMA, we may take L as 200 m (from Google Earth) and D as 12 m (from USGS survey data). Based on NOAA tidal predictions of the canal current under the Cape Cod Railroad Bridge, we may assign U_a values of 1.6 and 2.2 m s⁻¹, respectively, for neap and spring tides. The resulting estimate of through-canal volume transport is then 14 billion gallons for a neap tide (either flood or ebb) and 20 billion gallons for a spring tide.

To form a second estimate of tidal volume transport through the canal, we use a record of water velocity obtained from an Acoustic Doppler Current Profiler (ADCP) deployed in the canal as part NOAA's CMIST Program (see Section 3.7). The water depth and channel width at the deployment location (site 3 in Figure 10) are roughly 200 m (based on Google Earth) and 15 m (the ADCP deployment depth). Using these values for L and D above, and taking the vertically averaged ADCP velocity for $u(t)$, gives an

estimate of $F(t)$. Integrating the $F(t)$ time series gives a flood or ebb volume transport of roughly 16 billion gallons during a typical neap tide and 22 billion gallons during a typical spring tide.

A third volume transport estimate may be determined from the velocities output by the project's hydrodynamic model, SEMASS-FVCOM (see Section 3). Using these velocities, we computed the transport through a section of the canal roughly situated beneath the Cape Cod Canal Railroad Bridge. In determining the volume flux [$F(t)$ above], L and D were set to 200 m and 10 m, respectively, and $u(t)$ was taken as an area-average of the model-output velocity along the section. Integrating the volume flux time series gives a flood or ebb volume transport of roughly 14 billion gallons during a typical neap tide and 20 billion gallons during a typical spring tide, consistent with the two estimates above.

Based on these separate analyses, it may be assumed that the volume passing through the canal on a flood or ebb tide is order 14 billion gallons during ebb tides and order 20 billion gallons during spring tides.